

AD-A037 793

UNIVERSITY OF SOUTHERN CALIFORNIA LOS ANGELES ELECTR--ETC F/6 20/2  
RESEARCH STUDY IN GROWTH OF ALUMINUM-NITRIDE ON SAPPHIRE PIEZOE--ETC(U)  
AUG 76 K M LAKIN, J K LIU F19628-75-C-0098

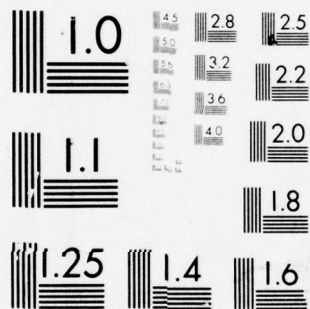
UNCLASSIFIED

RADC-TR-76-361

NL

| OF |  
AD  
A037 793





MICROCOPY RESOLUTION TEST CHART  
NATIONAL BUREAU OF STANDARDS-1963-A

ADA03793

RADC-TR-76-361



RESEARCH STUDY IN GROWTH OF  
ALUMINUM-NITRIDE ON SAPPHIRE PIEZOELECTRIC FILMS

FINAL REPORT

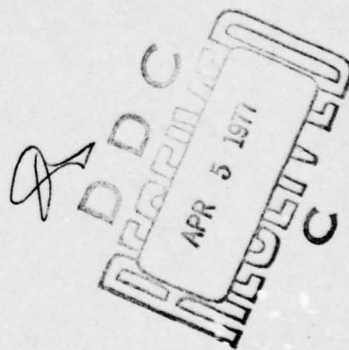
Kenneth M. Lakin

and

James K. Liu

Electronics Sciences Laboratory  
University of Southern California

COPY AVAILABLE TO DDC DOES NOT  
PERMIT FULLY LEGIBLE PRODUCTION



ROME AIR DEVELOPMENT CENTER  
AIR FORCE SYSTEMS COMMAND  
GRIFFISS AIR FORCE BASE, NEW YORK

AD NO. \_\_\_\_\_  
DDC FILE COPY

DISTRIBUTION STATEMENT A  
Approved for public release;  
Distribution Unlimited

K. M. Lakin and J. K. Lin are the co-principal investigators for this contract. Alan J. Budreau (ETEM), is the RADC/ETEM Project Engineer.

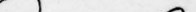
This report has been reviewed by the RADC Information Office (OI) and is releasable to the National Technical Information Service (NTIS). At NTIS it will be releasable to the general public, including foreign nations.

This technical report has been reviewed and approved for publication.

**APPROVED:**

Alan J. Budreau  
ALAN J. BUDREAU  
Project Engineer

**APPROVED:**

  
ALLAN C. SCHELL  
Acting Chief  
Electromagnetic Sciences Division

☒   
☐   
☐   
 SECTION   
 SUBSECTION   
 SECTION   
 SUBSECTION

FOR THE COMMANDER

UNDER *John V. Kues*



UNCLASSIFIED

SECURITY CLASSIFICATION OF THIS PAGE (When Data Entered)

1. REPORT DOCUMENTATION PAGE		READ INSTRUCTIONS BEFORE COMPLETING FORM	
1. REPORT NUMBER (18) RADC-TR-76-361	2. GOVT ACCESSION NO.	3. RECIPIENT'S CATALOG NUMBER (9)	
4. TITLE (and Subtitle) (6) RESEARCH STUDY IN GROWTH OF ALUMI- NUM-NITRIDE ON SAPPHIRE PIEZOELECTRIC FILMS.		5. TYPE OF REPORT & PERIOD COVERED Final Report. 1 Dec 74 - 31 Jul 76	
7. AUTHOR(s) (19) KENNETH M. LAKIN JAMES K. LIU		8. CONTRACT OR GRANT NUMBER(s) (15) F-19628-75-C-0098 new 1 Dec. 1974 to 31 July 1976	
9. PERFORMING ORGANIZATION NAME AND ADDRESS Electronic Sciences Laboratory University of Southern California University Park L.A. CA 90007		10. PROGRAM ELEMENT, PROJECT, TASK AREA & WORK UNIT NUMBERS Program Element 61102F 56350304 (12) (43)	
11. CONTROLLING OFFICE NAME AND ADDRESS Deputy for Electronic Technology (RADC/11) ETEM). Hanscom AFB, MA 01731 Attn: Alan J. Budreau		12. REPORT DATE August 76	
14. MONITORING AGENCY NAME & ADDRESS (if different from Controlling Office) (12) 77p.		13. NUMBER OF PAGES 75	
		15. SECURITY CLASS. (of this report) UNCLASSIFIED	
16. DISTRIBUTION STATEMENT (of this Report) Approved for public release; distribution unlimited		15a. DECLASSIFICATION/DOWNGRADING SCHEDULE	
17. DISTRIBUTION STATEMENT (of the abstract entered in Block 20, if different from Report)			
18. SUPPLEMENTARY NOTES			
19. KEY WORDS (Continue on reverse side if necessary and identify by block number) aluminum nitride, thin films, chemical vapor deposition sapphire substrates, surface acoustic wave			
20. ABSTRACT (Continue on reverse side if necessary and identify by block number) The growth and characterization of aluminum nitride epitaxial films on R- plane sapphire has been investigated in an eighteen month program aimed at improving the quality and uniformity of the material for use in microwave bandpass filters. This report details the entire process of AlN film processing starting from the polishing of sapphire wafers and ending with the electri- cal characterization of the resultant films. The polishing of sapphire → next page			

DD FORM 1 JAN 73 1473

EDITION OF 1 NOV 65 IS OBSOLETE

UNCLASSIFIED

SECURITY CLASSIFICATION OF THIS PAGE (When Data Entered)

361 620

next  
page

LB

UNCLASSIFIED

SECURITY CLASSIFICATION OF THIS PAGE(When Data Entered)

COM T

→ proved to be a major effort because the constraints of wafer thickness, optical flatness, wafer bowing due to thermal expansion stresses, and a defect free surface finish were not all compatible. Improvements were made in the AlN growth system and operating procedure which resulted in films of lower defect density, lower apparent strain, and improved acoustoelectric characteristics. Etching of the polished AlN surface followed by SEM examination was implemented as a means of checking crystal film perfection.

Measurements made on the temperature coefficient of delay of the film composite have shown values as low as 13 ppm for a thickness to wavelength ratio of 0.66 and indicate that zero temperature coefficient will be obtained at a somewhat larger thickness.



UNCLASSIFIED

SECURITY CLASSIFICATION OF THIS PAGE(When Data Entered)

## EVALUATION

1. This report is the Final Technical Report on the contract. It covers research done on the growth and testing of aluminum-nitride-on-sapphire piezoelectric films during the full period of performance. Aluminum-nitride-on-sapphire films were fabricated and forwarded to RADC/ET for use in the fabrication of surface acoustic wave (SAW) devices. Additional testing was performed at RADC/ET and given back to the University of Southern California. Advances were made in understanding, but not completely solving, problems associated with the fabrication of such films.

2. SAW devices are finding increasing use in military and other systems due to their advantages of small size and weight, low cost and reliability. Aluminum-nitride-on-sapphire, with its velocity approximately twice that of other materials, will allow SAW devices to operate at twice the frequency previously possible.

*Alan J. Budreau*

ALAN J. BUDREAU  
Project Engineer

## TABLE OF CONTENTS

1.0	INTRODUCTION .....	1
1.1	Background .....	1
1.2	Program objectives .....	2
1.3	Research tasks .....	2
1.4	Accomplishments .....	3
2.0	EXPERIMENTAL DETAILS .....	5
2.1	Substrate preparation .....	5
2.1.1	Conventional polishing with "soft" laps .....	9
2.1.2	Pitch lap polishing .....	9
2.1.3	Modified RCA "preferential" polishing .....	12
2.1.4	Polishing on platens with adjustable profiles ..	14
2.2	Aluminum nitride film growth .....	18
2.2.1	Growth reactions .....	20
2.2.2	Growth system .....	21
2.2.3	Optimization of growth system .....	25
2.2.3.1	Characterization of injection systems .....	25
2.2.3.2	Water cooled reaction chamber .....	29
2.2.3.3	Effect of silicon upon AlN growth .....	32
2.3	Sample preparation .....	35
2.3.1	Sample mounting for polishing .....	35
2.3.2	Film polishing .....	38
2.4	Film characterization .....	39
2.4.1	Film thickness measurement .....	40
2.4.2	Electrical characterization of films .....	40
2.4.2.1	Discussion of $K^2$ and $V_s$ measurements .....	44



2.4.2.2	Surface-wave group velocity .....	51
2.4.2.3	SAW attenuation in film .....	54
2.4.3	Other experiments .....	57
2.4.3.1	Film etching .....	57
2.4.3.2	Sample bowing due to thermal effects .....	57
2.4.3.3	Temperature coefficient of delay .....	61
3.0	CONCLUSION AND RECOMMENDATIONS .....	64
3.1	Conclusions .....	64
3.2	Recommendations .....	65
	REFERENCES .....	67



# LIST OF ILLUSTRATIONS

FIGURE	PAGE
1. Exaggerated view of sapphire wafer distortion.....	8
2. Conventional polishing system.....	10
3. Pitch lap polishing system.....	11
4. Modified "preferential" polishing system.....	13
5. "Adjustable" platen polishing system.....	16
6. Deflection of a solid circular plate under pressure.	17
7. AlN epitaxial film growth system.....	22
8. As-grown AlN surface morphology of different film thicknesses.....	24
9. A "hot-wire" generator.....	27
10. Injection tube gas flow velocity profiles.....	28
11. Water cooled reaction chamber.....	31
12. Surface morphology of AlN 09247410.....	33
13. SAW measurement data of AlN 09247410.....	34
14. AlN growth with injected SiH <sub>4</sub> .....	36
15. Reflected impedance Smith chart plots.....	42
16. Electromechanical coupling constant,..... K <sup>2</sup> , versus t/λ .....	46
17. Surface acoustic phase velocity, V <sub>s</sub> versus t/λ .....	47
18. Surface morphologies of some AlN samples.....	48
19. Surface wave group and phase velocities versus t/λ .	52
20. SAW transmission versus frequency.....	53

21. Character of polished AlN film surfaces under some IDT's. ....	55
22. Some etched AlN surfaces. ....	58
23. Growth transition area on AlN film. ....	60
24. Temperature coefficient of surface wave delay versus film thickness. ....	62

## 1.0 INTRODUCTION

### 1.1 Background

Aluminum nitride epitaxial films grown on R-plane sapphire are of interest for microwave frequency surface acoustic wave (SAW) devices, such as frequency bandpass channel filters, because the high velocity of propagation, 6 km/sec, implies a reduction in photofabrication requirements by a factor of two over quartz. Further the high coupling coefficient of 0.8 percent suggest lowered filter insertion losses.

Other important factors are associated more with the substrate. First, the R-plane of sapphire is also used for the growth of epitaxial silicon and consequently allows hybrid fabrication of SAW filter and integrated circuit switching elements for the implementation of monolithic circuit elements. Second, R-plane sapphire is an increasingly less expensive substrate due to its use in the production of silicon-on-sapphire integrated circuits. Third, the large area substrates promise AlN films covering areas in excess of 10 square inches; a number unlikely to ever be achieved by bulk wafers because the largest bulk AlN samples measure in the 1-3 mm range. Finally, more recent results have shown that the AlN-on-sapphire composite exhibits a temperature coefficient of delay of as low as 13 ppm for a film thickness-to-wavelength ratio of 0.66.

At first glance then, this material combination appears to

be very desirable. However, it is not without its problems when it comes down to producing the high quality material required by microwave frequency SAW filters. Specifically, the real problem areas are film thickness uniformity, strain induced warping of the substrate which causes device fabrication errors, and coupling coefficient and propagation velocity variations due to imperfections in the film microstructure. The causes of these problems involve a complicated interplay between pre-growth preparation of the sapphire substrate, the actual growth conditions in the epitaxial reactor, post-growing of the film, and subsequent regrowth operations wherein AlN is the substrate. These problems were investigated in the course of the research project and are described in the following report.

### 1.2 Program objectives

In general terms the goal of the research project was to conduct the necessary research required to solve the problems associated with the fabrication of AlN and to then produce a limited number of representative samples for use at RADC/ET in the microwave frequency filter program. Early in the program this broad objective was reduced to a set of specific experimental research tasks which are outlined below and discussed in greater detail in Section 2.

### 1.3 Research tasks

The specific research tasks that were defined in order to

carry out the research objective are i) substrate preparation ii) aluminum nitride film growth iii) sample preparation iv) and film characterization. The first task was undertaken in order to meet the requirements of optically flat finished material samples using thick substrates. The second task involved a study of the gas injection system and its effect upon the growth uniformity of the AlN films. The goal was to find those conditions which would create more reproducible acoustic characteristics and flatness uniformity in the as-grown films. The third task involved the relatively difficult problem of polishing. Here it was necessary to meet not only the flatness requirement but also to maintain the thickness uniformity of the film itself. The fourth task involved the actual fabrication of UHF transducers and from measurements made upon the transducers evaluate the coupling coefficient and propagation velocity of the film-substrate composite.

#### 1.4 Accomplishments

The overall accomplishment of the program was the definition and verification of the procedures for fabricating high quality AlN films of the type required for microwave frequency filters and to deliver a limited number of these samples to RADC/ET for further evaluation. Specifically, it was found that films of optimum quality and consistency are best achieved using a horizontal slotted arm vertical injection system. Further, it was found that film and substrate polishing in preparation for



AlN growth is best done with a chemo-mechanical polish which produces a surface with little damage.

Acoustoelectric evaluation of the films provided significant data to add to that already obtained and has verified the desirable properties of this material. The problems of interfacial strain and rapid coupling coefficient roll off at thinner film thicknesses were clarified.

## 2.0 EXPERIMENTAL DETAILS

### 2.1 Substrate preparation

One of the requirements of the goals specified in the contract was to produce samples with surfaces flat to within two optical wavelengths ( $\lambda = 6000\text{\AA}$ ) flatness. This effectively requires substrates with very tight dimensional tolerances.

The aluminum nitride-film-on-sapphire composite is known to be under considerable strain due to the lattice and thermal coefficient of expansion mismatches [1]. The effect is manifested in the bowing of substrates after film growth with the AlN on the convex surface, and/or in film or substrate cracking [2,3,4]. With the specified sample dimensions and improved growth conditions [5], however, minimal substrate bowing and cracking was seen in our samples. Nevertheless, though the visible effect of strain was minimized through use of small and rigid substrates and improved growth methods, the effect taken together with surface rounding, caused by conventional polishing methods and nonuniform growth rates, combined to produce sample surfaces out of tolerance. It is clear then, that the goal of producing flat samples can only be achieved by working on all phases of the fabrication of the substrate preparation through film growth and film preparation to achieve the program goals.

The R-plane (01 $\bar{1}$ 2) sapphire wafers used for substrates in the program were purchased from Union Carbide in lots. Use of 3" diameter wafers, although they cost less per unit area than 1.5" wafers, was dropped in favor of the smaller wafers for AlN growth. The larger wafers presented more problems in that their surfaces were more "out of flat" required more work in surface preparation than the smaller wafers.

The wafers purchased had the orientation flats (0.5" in length) oriented perpendicular to the sapphire [01 $\bar{1}$ 1] direction rather than along 45 degrees as normally used for silicon on sapphire in order to prevent ambiguities and consequently additional substrate orientation work as far as the [01 $\bar{1}$ 1] direction is concerned. These flats were specified to within 1 degree and this was confirmed by X-ray analysis.

Wafers of two surface finishes were purchased for this program. Most of the wafers were purchased with epi-quality surfaces. The surfaces were prepared at Union Carbide with a final polish using Syton [6] a chemo-mechanical polish of colloidal silicon dioxide suspended in an alkaline fluid. The wafers exhibited excellent surfaces with minimal mechanical damage but rounded to figures of about 20 optical wavelengths per diameter inch. A number of wafers were also ordered with "mirror" finishes. These had surfaces that had undergone final diamond slurry polishing (grit size 5 microns) in preparation for the Syton polishing step. The wafers exhibited better surface

flatness than those with "epi-quality" surfaces but had damaged surfaces unsuitable for epitaxial growth without further surface preparation.

The surfaces of the wafers actually exhibited more complex contours than hemispherical convex shapes usually associated with polished surfaces. The predominant surface contour was one resembling a "saddle" or "potato-chip"-like shape, (Fig. 1). This effect can be seen in all wafers in various degrees of severity. The effect was easily seen from the eccentricity of the interference fringe patterns obtained between a one-tenth wave optical flat and the wafer surface. This effect is probably due , i) the polishing process which involved high loads in mechanical mounting and polishing, and ii) the anisotropic polishing effect in the R-plane of sapphire. The "potato chip" effect was pronounced enough in some wafers to effectively present concave surfaces, contrary to the normally expected convex surfaces usually associated with polishing methods.

It was in the interests of the final project goals to achieve substrates with surfaces that are flat to within two optical wavelengths or with slightly concave surfaces (to compensate the bowing effect of the strain induced by the AlN films to be grown on the substrates). The preparation methods used on the wafers for the project are listed in the following sections.

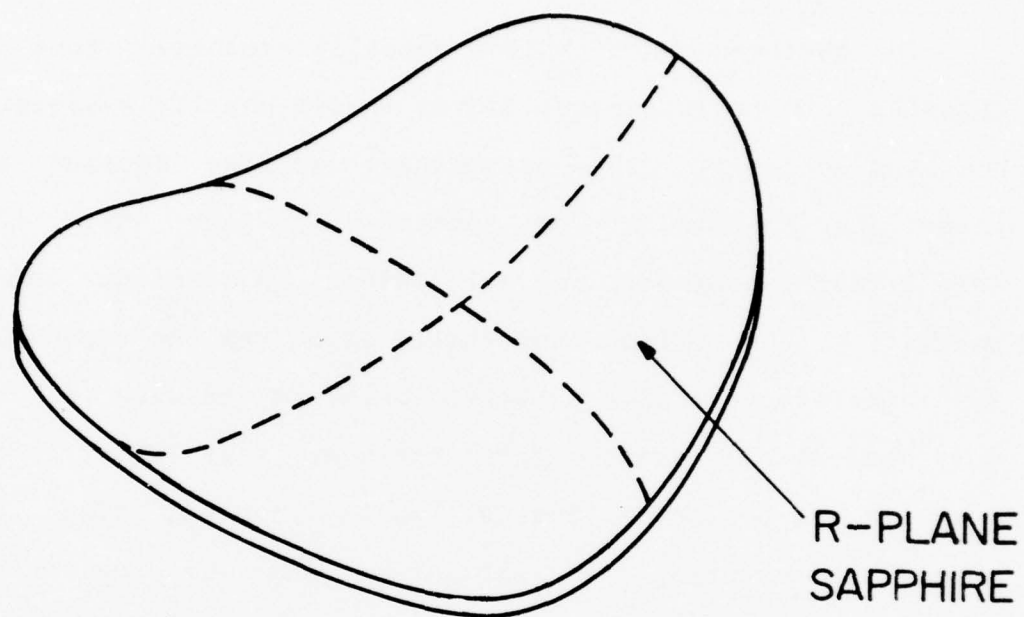


Figure 1. Exaggerated view of sapphire wafer distortion.



2.1.1 Conventional polishing with "soft" laps. Wafers of surface profiles showing more than two wavelengths per inch off-flatness are mounted onto a stainless steel polishing blank with wax (Apiezon Z). If multiple wafers are mounted they are distributed evenly in a circular pattern. These wafers were polished over periods of up to 30 hours on a conventional polishing apparatus using Syton as the polishing agent and Corfam [7] for the polishing cloth, (Fig. 2). The surfaces were constantly monitored with a quarter-wave optical flat.

The mounting procedure for the wafers is an important step in achieving the desired result; any stress put on the wafers in mounting would result in wafers with non-flat surfaces after dismounting and the stresses having relaxed. In the case of multiple wafers, the wafers also had to be mounted coplanarly to ensure even polishing of all surfaces. Improvements in surface flatness were obtained mostly with wafers that were concave initially. This is probably because of the equipments tendency to preferentially polish at the edges of the wafers rather than at the middle.

2.1.2 Pitch lap polishing. An attempt was made to adapt the technique used to polish mirror blanks to polish sapphire with Syton. A pitch lap was fashioned out of optical polishing pitch, a hexagonal lapping mold and a 12" diagonal  $1/4$  wavelength optical flat, (Fig. 3). However, Syton did not have sufficient grit volume to prevent the pitch lap and the wafers from rubbing

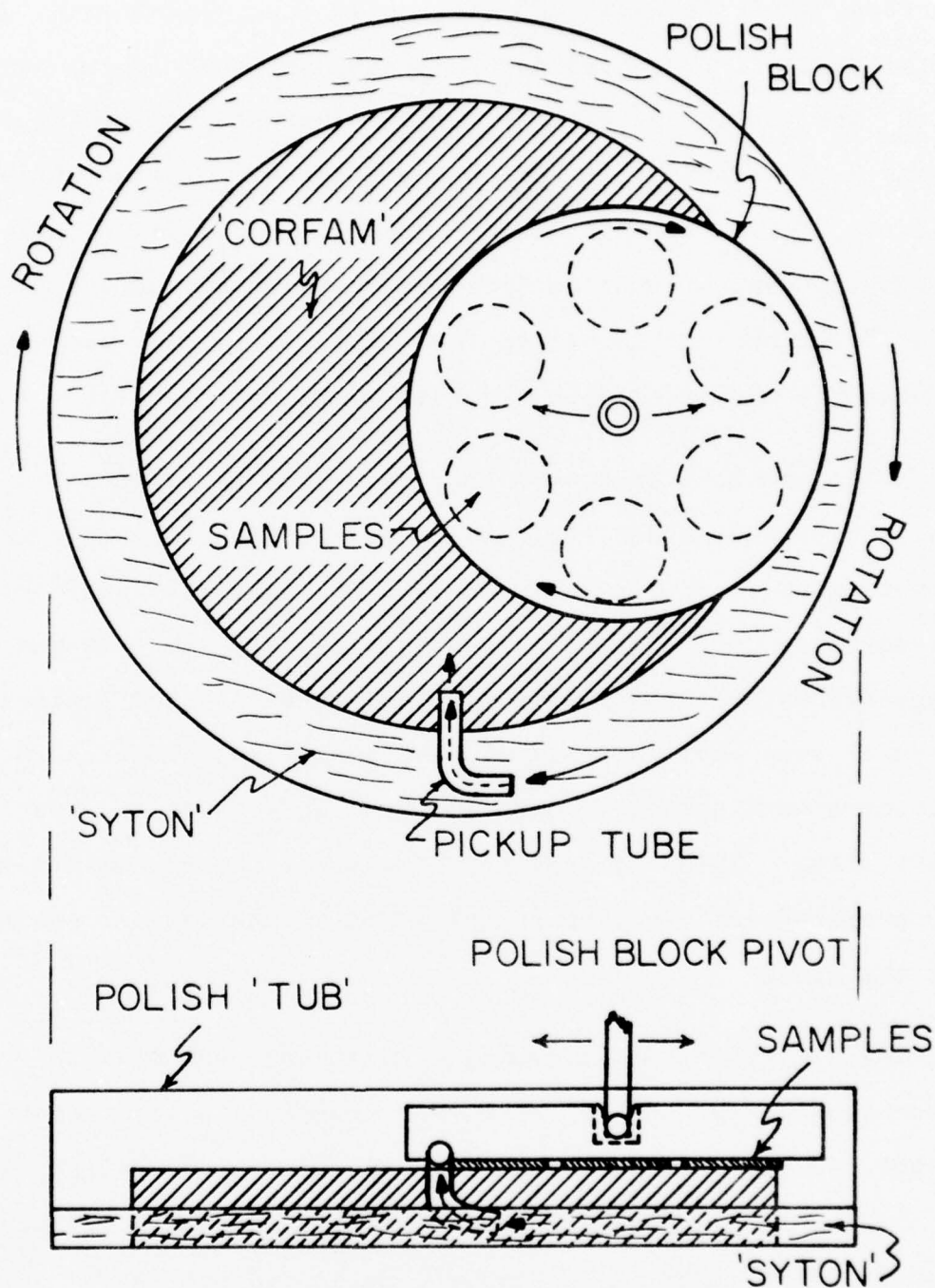


Figure 2. Conventional polishing system.

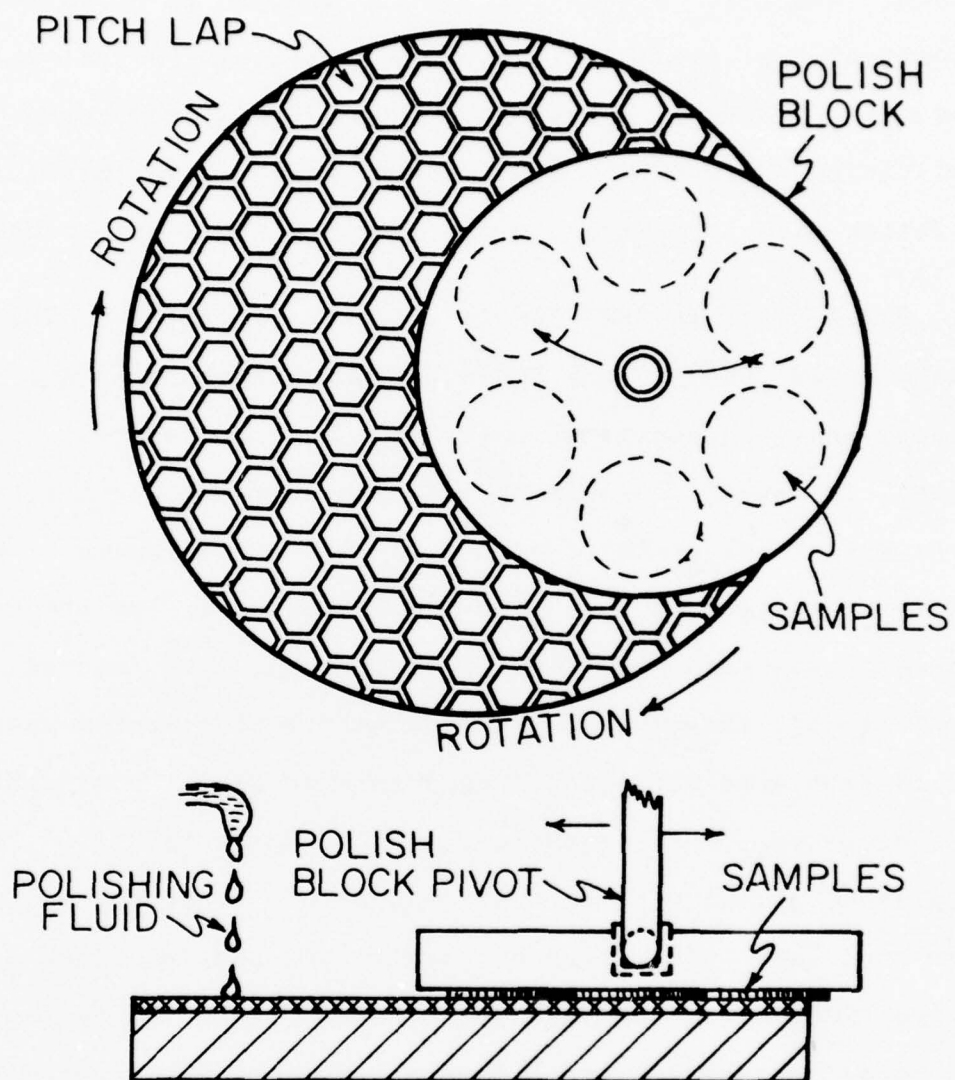


Figure 3. Pitch lap polishing system.

together and destroying the lap surface. Consequently, the attempt was not successful. (It should be noted that using mechanical-type polishes like Linde "A", would conceivably have produced flatter substrates but the requirement of an "epi-finish" surface for AlN growth would have meant further polishing with Syton is required...making the point academic).

2.1.3 Modified RCA "preferential" polishing. The polish pads (Corfam) used in the Syton polishing techniques are soft and porous, hence conventional polishing methods wherein polishing action is equal throughout a sample surface cannot improve the surface flatness of the samples. A technique wherein material removal rate decreases with radial distance from the center of the wafer was required for correction of the convex surface profiles of the wafers. The concentric ring system used by RCA [8] is such a method and was used as a model for our preferential polish setup. The polishing setup, as shown in Fig. 4, features a polished platen with an inner and outer ring of Corfam that supported and also helped rotate the sample holder which was allowed freedom to rotate about a fixed pivot. Polishing action was provided by a ring of Corfam between the two rings. It had serrated edges and was set off center on the polish platen to prevent discontinuities in polish action across a wafer surface. Syton was recirculated onto the polish pad surface with a centrifugal pick up tube.

The polishing action profile across a wafer surface for this

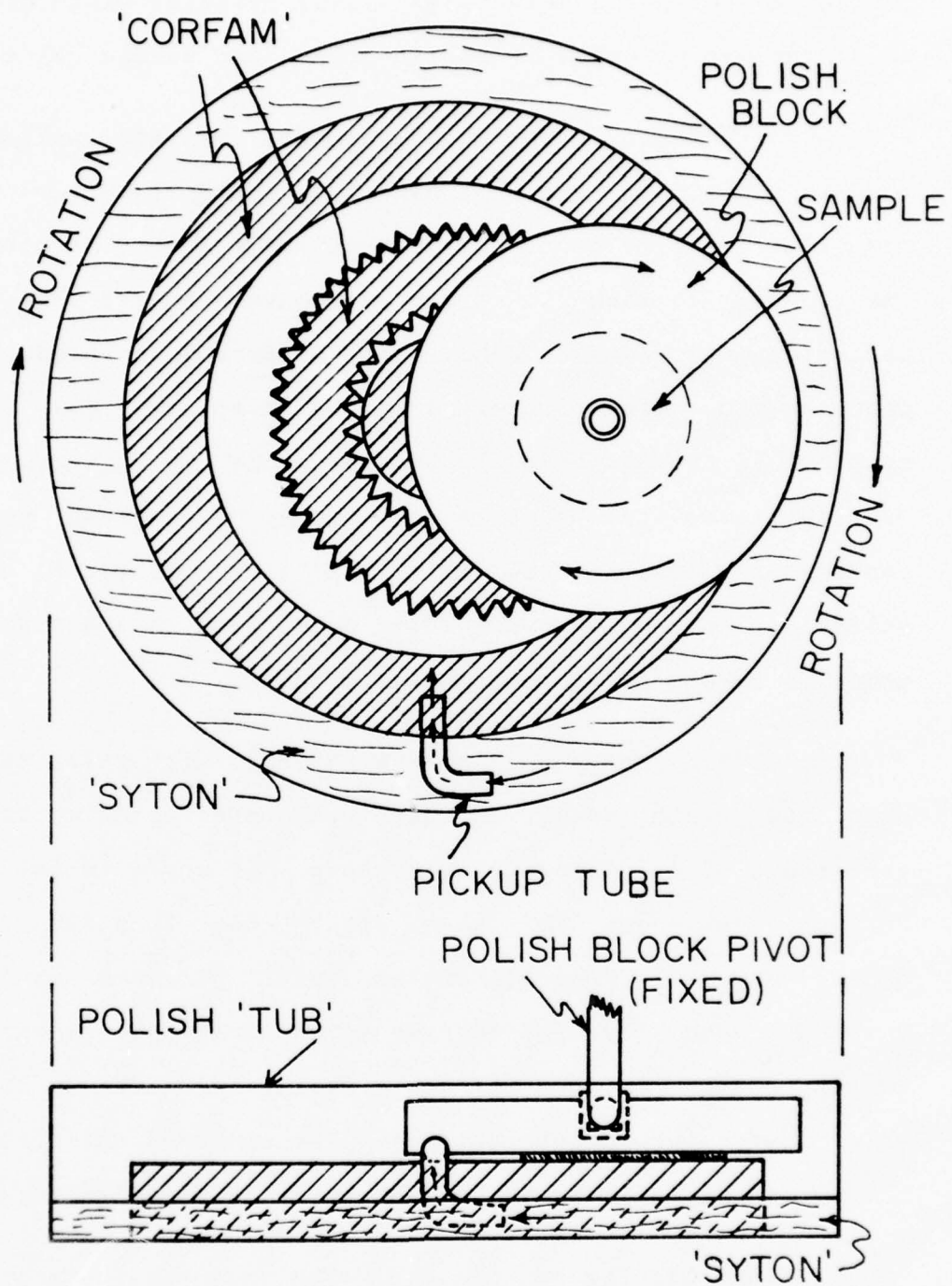


Figure 4. Modified "preferential" polishing system.



polishing setup is determined by, i) relative width of the size of serrations on edges of polish platen and sample holder.

Disadvantages of the technique are, i) the polish action profile sometimes did not match up to sample surface curvature such that a sample could have the center region flattened before the edges, leading to a concave-convex surface with continued polishing, ii) pad widths had to be different to produce polish profiles to match different sized samples, iii) it was not apparent if the method could be applicable to irregular shaped samples and, iv) surface curvature of samples had to be continuously monitored as this was a "corrective" method of polishing and any over-polishing would lead to substrate surface profiles as bad or worse than the original.

Some 3" diameter wafers were polished with this method and with pad width equal to half the wafer diameter having edge serrations of  $1/6$  wafer diameter deep. At approximately 2 psi, surface flattening was seen after about 20 minutes of polish time. However, discontinuities still occurred in polishing action around the polish ring edges as was seen in the surface profile of the polished wafers. Flattening across the entire wafer surface was not achieved. The problems being mainly that of the discontinuities in polish action and disadvantage (i).

2.1.4 Polishing on platens with adjustable profiles. A different approach to the polishing problem was formulated. A hollow polishing wheel for the polishing machine was constructed

so that the profile of the polishing surface can be changed anywhere from that of a flat surface (as is the normal profile of all conventional polishing wheels) to a convex or a concave surface by application of either pressure or vacuum to the hollow cavity in the wheel (Fig. 5). It is hoped that this approach to the polishing problem could compensate and eliminate the inherent tendency of all rotary polishing fixtures to impart a convex surface to a polished sample. The approach should be excellent particularly in the case of chemical polishing with soft polish pads.

The deflection of a solid circular plate under pressure has been calculated for different physical configurations, materials and plate thicknesses [9]. For our case, the formulas for deflection are

$$y = \frac{KWa^2}{Et^3} = \text{deflection}$$

$$W = wrr^2, \text{ total pressure, psi}$$

(assuming  $a/r = 1$ , Poisson's ratio = 0.3)

$K$  = loading support factor for deflection

= 0.212 case (a), Fig. 6

= 0.053 case (b), Fig. 6

$t$  = thickness of plate in inches

$E$  = Young's modulus =  $3 \times 10^7$  psi for steel

This means that for a 10" diameter steel plate with hollow top of about 0.25" thickness, a pressure of 50 psi would cause a

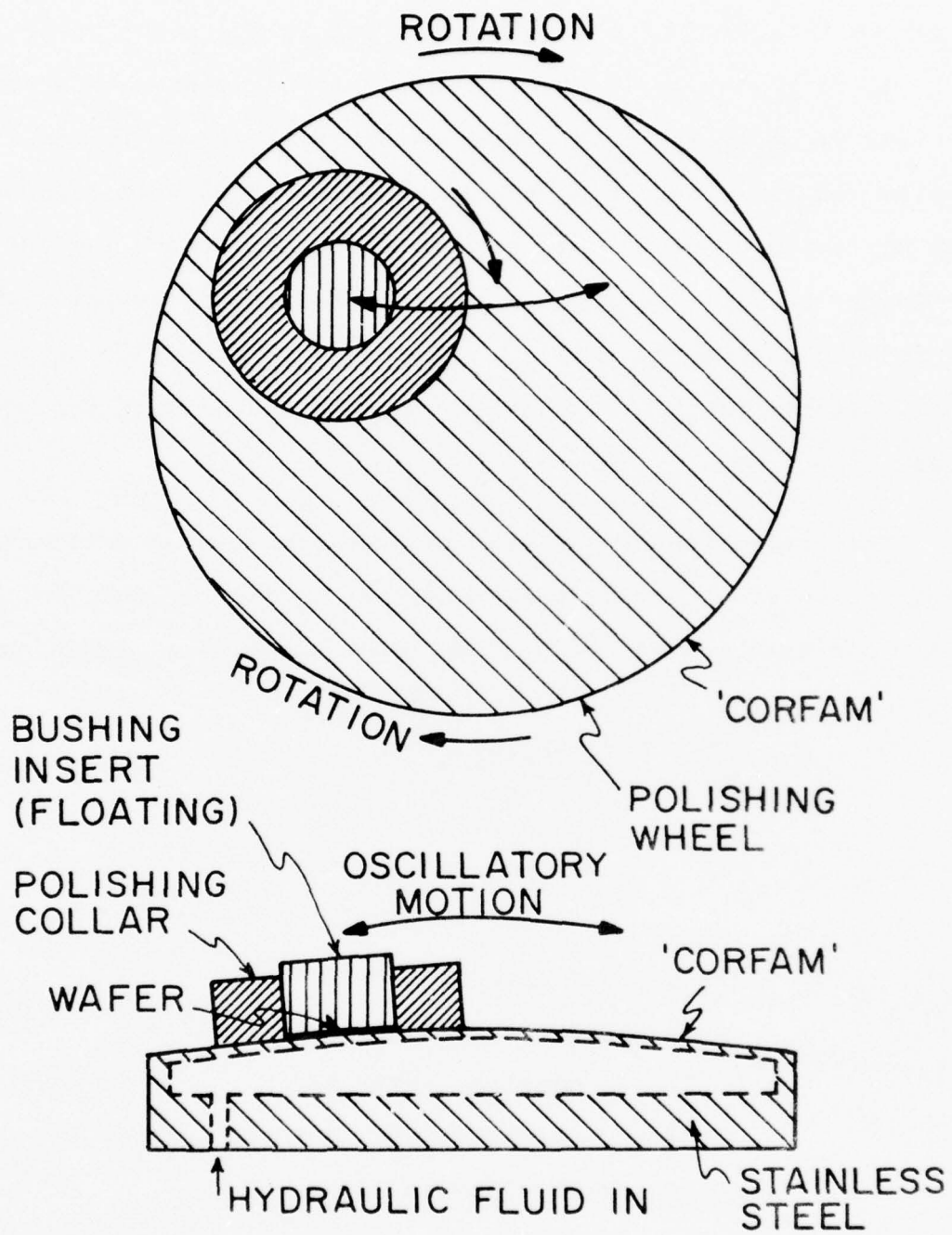


Figure 5. "Adjustable" platen polishing system.

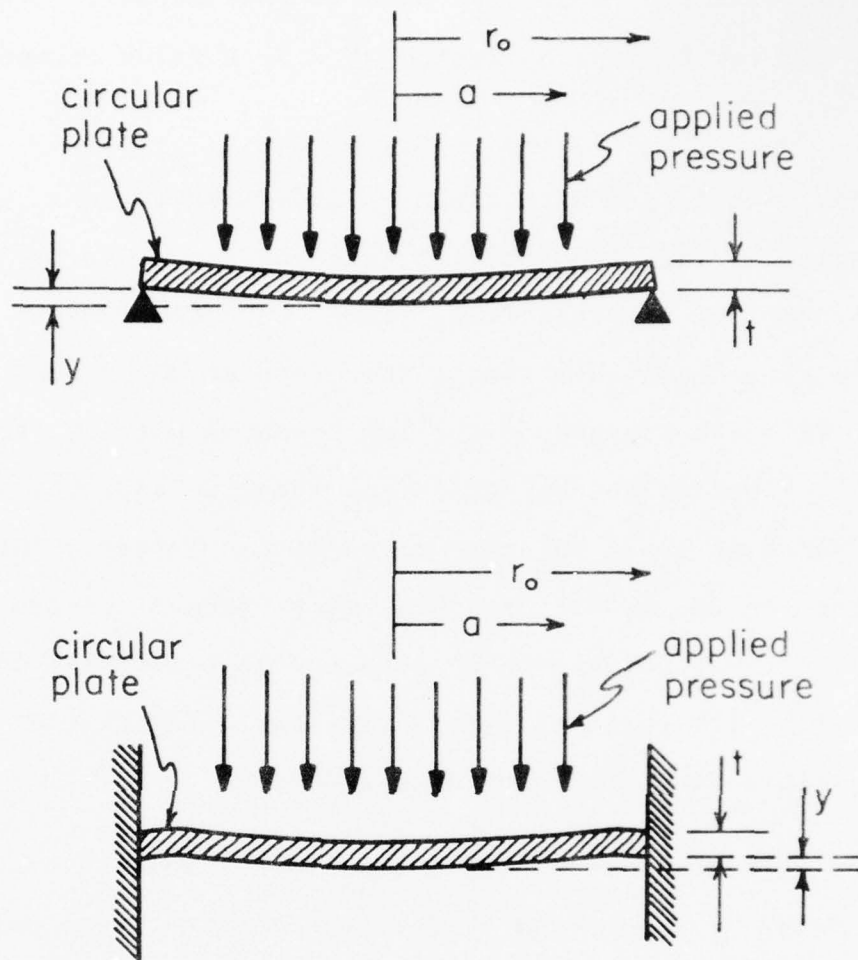


Figure 6. Deflection of a solid circular plate under pressure.

deflection of approximately 25 mils at the center, the loading support factor K being estimated at 0.1, a value between cases a and b.

Results obtained with sapphire wafers have been mixed but encouraging. The tendency of the wafers to be polished to a concave profile is definitely seen but the amount of time required to achieve this was of the order of 30 or more hours per wafer. This was because of the low pressure put on the polish blank ( 4 psi). Union Carbide polishes the sapphire with Syton at pressures at least an order of magnitude larger. The present polishing setup cannot achieve much larger pressures on the samples. It was shown however that the objectives of the method were met, with polished wafers that exhibited flatter surfaces, albeit with a very time consuming process.

The applicability of the method to polishing irregular size samples made it especially well suited for the final polishing of AlN films on sapphire. Here the rate of polishing was much higher and results were obtained in the order of minutes, (See Section 2.3).

## 2.2 Film Growth.

The basic growth technique of AlN films on sapphire used in this study was that of chemical vapor deposition (CVD). As a rule, CVD processes are inherently very complex and while there have been some previous studies of specific CVD mechanisms, most



of the systems are poorly understood.

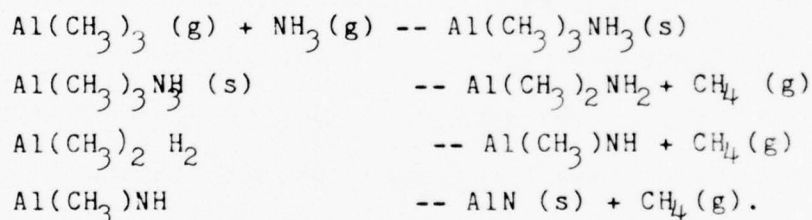
For a typical CVD growth process, a convenient working model for kinetic factors affecting growth is that of assuming a boundary layer above the substrate surface where the gas stream velocity approaches zero. This layer defines a concentration gradient of reactant gases from the main stream value to the equilibrium concentration value at the substrate surface. This is the driving force for epitaxial growth that promotes the diffusion of reactants and gaseous end products of the reaction at the surface through the boundary layer.

For a finite layer thickness then, the rate limiting step for epitaxial growth is mass-transport and therefore physically controlled. Improving gas dynamics around the substrate surface would promote film growth. However, by increasing the gas flow the boundary layer decreases to a point where the concentration of the reactants at the substrate surface approaches that of the main stream value. Now the growth rate is limited or determined by a surface process and is said to be surface or reaction kinetics controlled. The limiting rate at the surface may be due to reactant absorption, product desorption or actual chemical reaction.

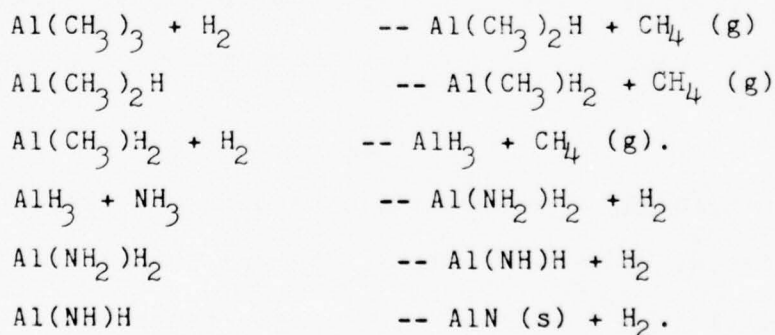
Thus, depending upon the gas transport efficiency and rate of the epitaxial growth processes, CVD growth rate can be limited by a combination of either or both mass transport or reaction kinetics controlled processes.

2.2.1 Growth Reactions. AlN in this project was grown via a CVD process involving the reaction of trimethylaluminum (TMA) and ammonia as sources of aluminum and nitrogen respectively. The use of TMA and ammonia in the presence of hydrogen (as carrier gas) at high temperatures for growth of AlN suggests a complex reaction chemistry. Reactions leading to AlN solid formation can involve the hydrogen gas well as the components of the two reactant gases. The reactions are further complicated by the fact that TMA reacts with ammonia at room temperature to form a solid compound,  $(\text{CH}_3)_3\text{Al}:\text{NH}_3$  which de-alkalyzes with increasing temperature to finally release AlN as a solid [10]. Some of the possible reactions leading to AlN formation in the growth system are listed below:

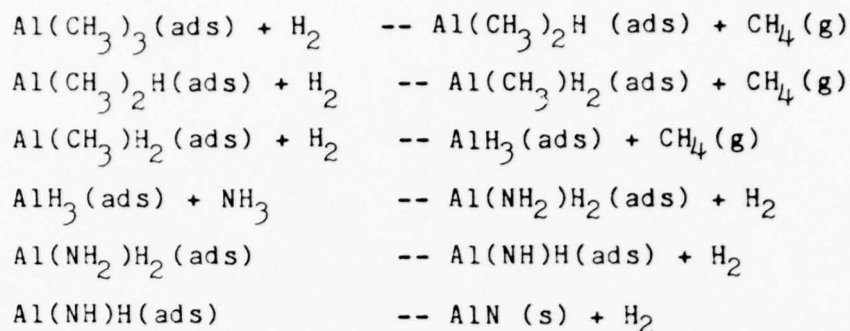
#### Reactions I



#### Reactions II



#### Reactions III



The third group of reaction, where the reactions occur at the substrate surface where TMA is absorbed, is probably unlikely in view of the fact that TMA is a very volatile gas hence reactions 1 or 2 would probably predominate.

2.2.2 Growth system. The basic growth system for AlN films on sapphire is that of an epi-reactor modified to handle metalorganic gases, Fig. 7 (From [5]). The gases are brought in from the center of the susceptor. The rapid reaction between TMA and NH dictates the separation of the incoming gases by a coaxial arrangement and the physical direction of the gases onto the substrate surfaces away from the hot reaction chamber walls.

The gases are injected through an injection slot cut at the bottom of a horizontal arm projecting from the quartz injection tube. This enables growth of AlN films over the entire area of a 1.5" diameter sapphire wafer, by oscillating the susceptor so that the entire sample surface is exposed to the injected gases. The approximate growth rates for good AlN films range from about 1  $\mu$ /hr. to 3  $\mu$ /hr.

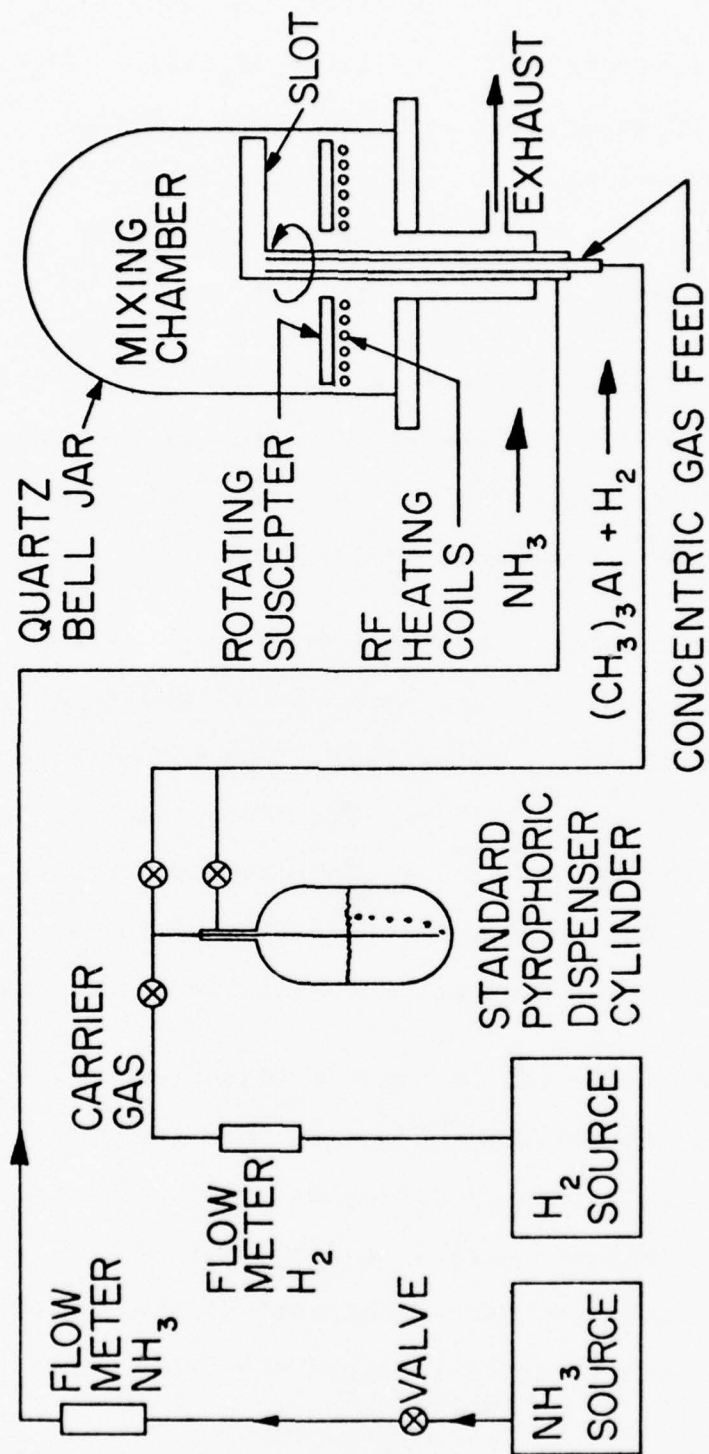
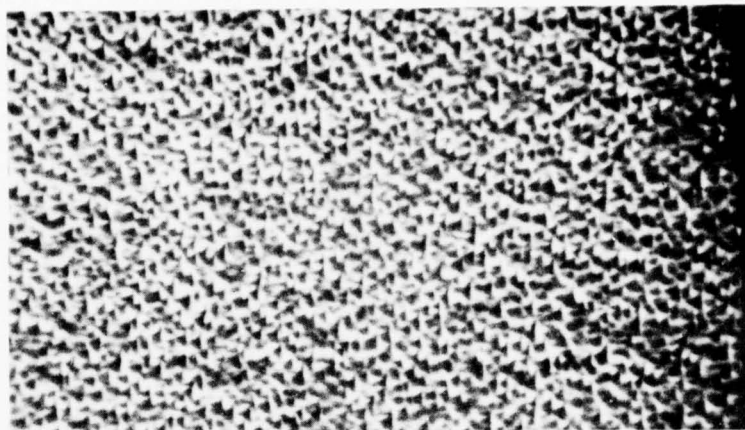


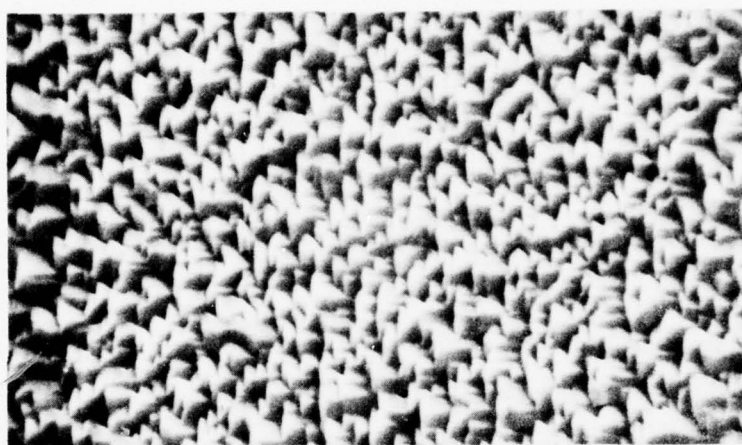
Figure 7. AlN epitaxial film growth system.

Growth times were limited because the AlN surface morphology became progressively rougher and defects (as in inclusions and holes in growth surface) increased in number as well as size with increasing film thicknesses of much beyond 5  $\mu$ , Fig. 8. The growth periods were short also because the injection system had a tendency to clog the injection slot with AlN polycrystalline overgrowth. This resulted in uncontrolled flow profile changes and pits and spurious nucleations forming on the surfaces because of dislodged overgrowth. At a total gas flow of approximately 10 l/min, calculated average gas velocities in the quartz coaxial tube are about 31 cm/sec while velocities of gases from the injection slot can run higher. High flow rates of the gases were required for growth of the AlN film. Several possible explanations for this come to mind: i) Growth is mass-transport limited and a high gas velocity is required to reduce the boundary layer to a point where growth proceeds at reasonably fast pace, ii) Experiments have been made on epitaxial film growth to show that if growth temperatures were varied to allow for alternate melting and recrystallization of the nucleating material, better and more coherent growth was achieved [11]. Temperatures on the substrates under the high flow of the cold gases do differ from that of the susceptor. This would be a function of the exposure time for that particular sample region to the gases (i.e. susceptor oscillating frequency), flow volume, velocity of the gases, and substrate thickness.

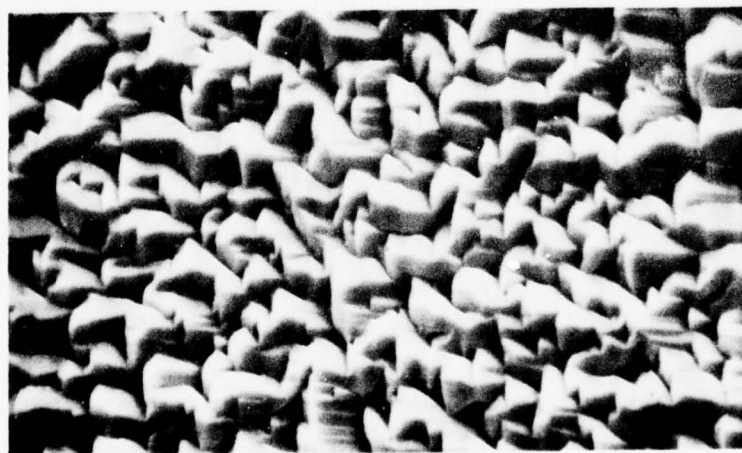




a)



b)



c)

Figure 8. As-grown AlN surface morphology of different film thicknesses.

Temperature differentials on the substrates under actual growth conditions were hard to measure because of the use of an optical pyrometer for temperature measurement and because of the substrate's transparency. However, the darkening of the hot susceptor surface, when under constant flow of the injected gases, indicate that temperature differentials would be in the order of 50°C or so. iii) The rapid reaction of TMA with NH indicates that for the gases to be able to react at the substrate surface, gas velocity has to be sufficient to propel the gases to the surface before premature completion of the reaction in the hot reactor atmosphere. iv) The injection tube being physically located vertically above the sample surface, means that the injected gases need sufficient velocity to overcome the convection currents caused by the heated susceptor.

2.2.3 Optimization of growth system. Several experiments were performed on the growth apparatus in attempts to optimize growth conditions.

2.2.3.1 Characterization of injection systems. Growth rates of the AlN film were very dependent on the particular injection tube used for the run. This points to the necessity to characterize the injection tubes in order to understand the flow profiles of gases present at the substrate surface.

A simple hot-wire anemometer probe utilizing a Cr-Al thermocouple and tungsten heater wire was constructed. The anemometer functions by correlating gas flow velocity with a

change in temperature of the heated air surrounding the thermocouple. This probe was placed in the growth apparatus and various injection tubes were characterized as to their flow profiles, Fig. 9. Measurement conditions were not identical to growth conditions since measurements were done at room temperature where gas viscosity is low and convection currents due to the heated susceptor surface were missing. However, a good qualitative view of the flow profiles can be seen along with the opportunity to compare different injection systems.

Gas flow profiles of injection tubes of different configurations were measured with the hot-wire anemometer, Fig. 10. In general, the profiles confirmed previously held impressions of the nature and distribution of gas flows on the different systems.

The vertical injection system (i.e. tube V, Fig. 10), as used for SOS growth in industry, provided very even and consistent flow profiles of the different systems from injection tube to injection tube. Its advantages also include the fact that the velocity profile is uniform throughout the susceptor surface, allowing constant rotation of samples during growth without having to resort to oscillating the sample as is required for the injection systems directing gas flow onto the susceptor surface. Its disadvantages however, turned out to be insurmountable for AlN growth where very high gas flow rates are required for the vertical injection system in order to produce a

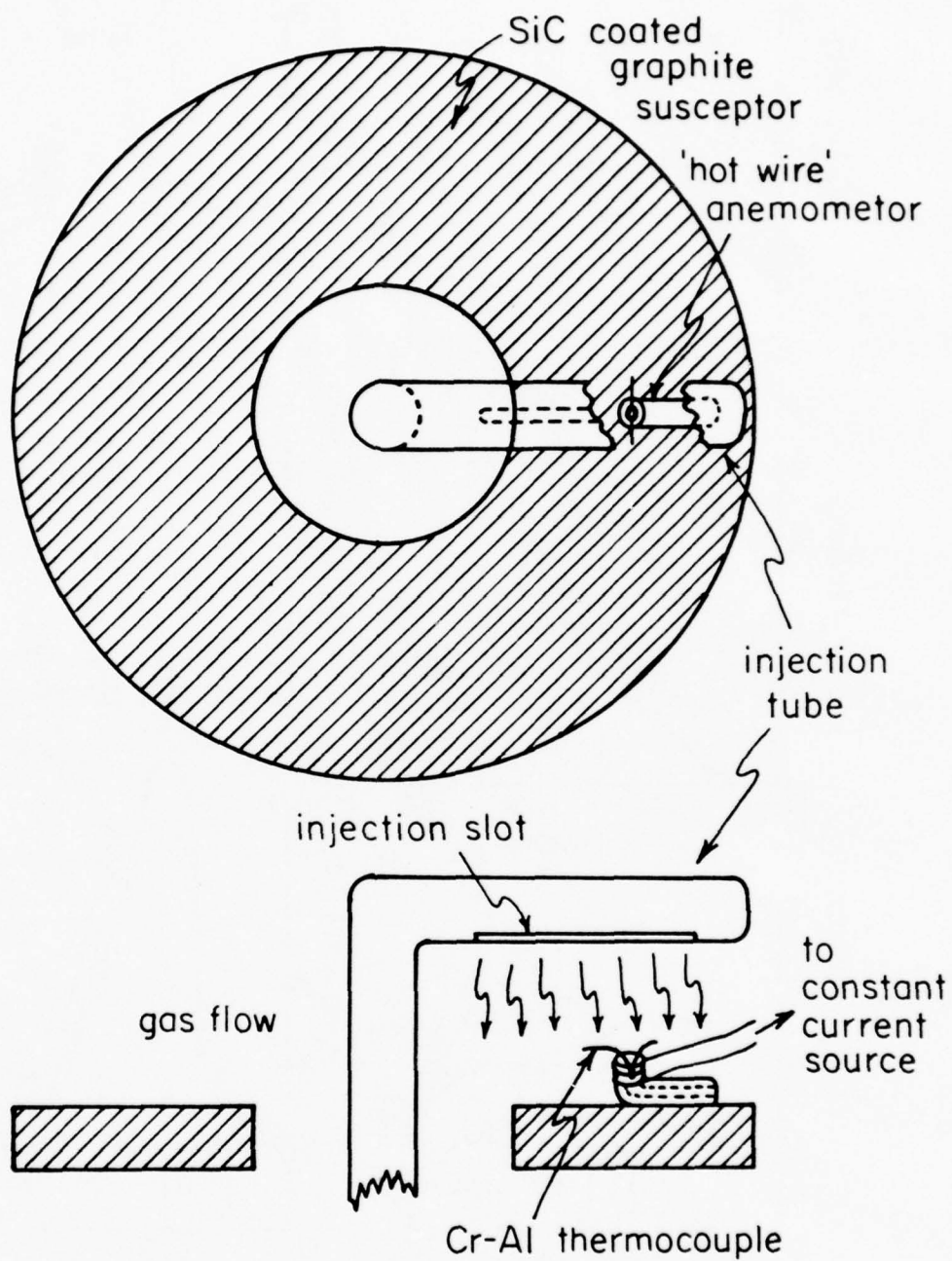
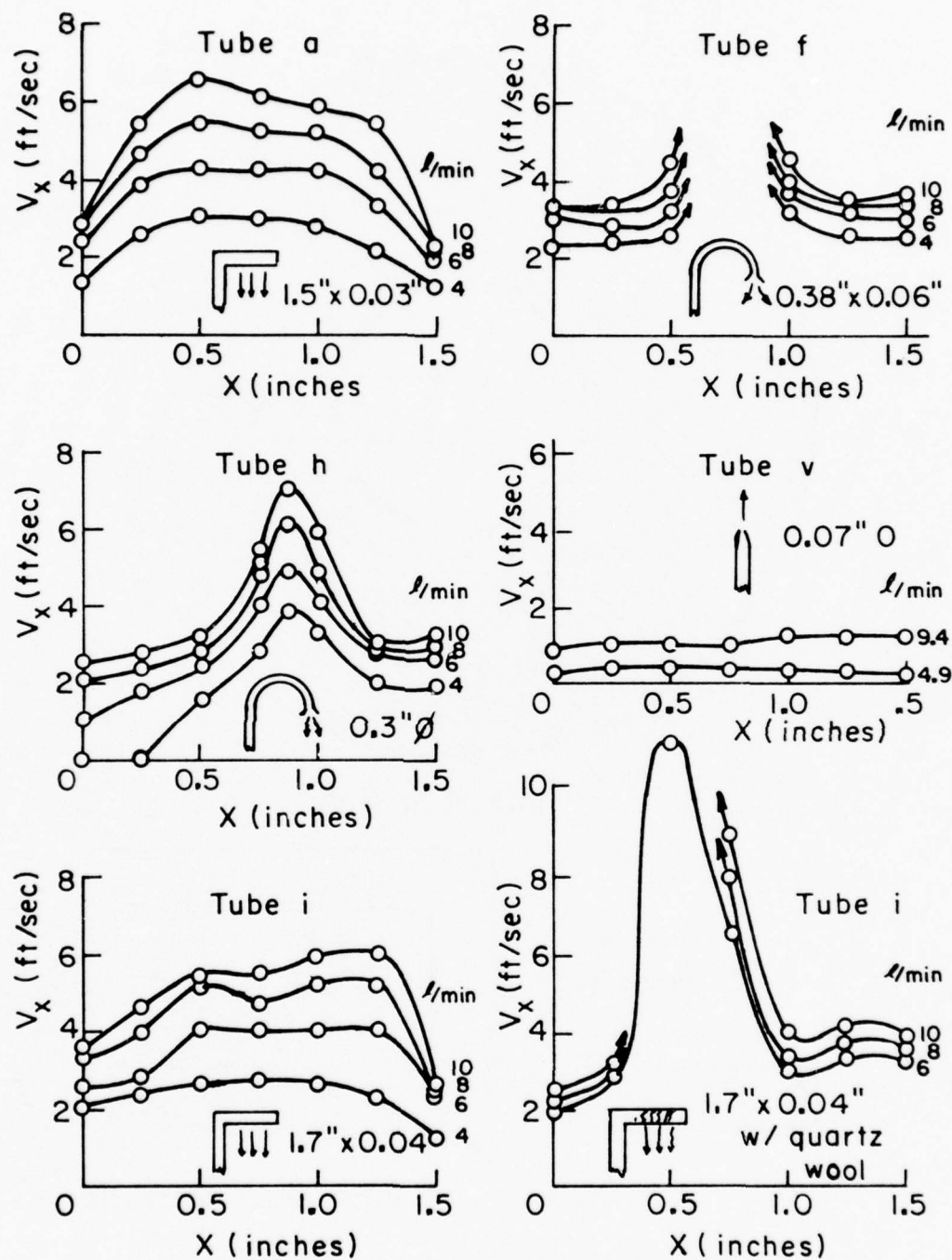


Figure 9. A "hot-wire" generator.



$X$  = horizontal distance at substrate surface

Figure 10. Injection tube gas flow velocity profiles.



gas velocity at the substrate surface. Most important, however, was the disadvantage that the reactant gases had to travel a large distance (and hence a long time) before reaching the substrate surfaces and are in constant contact with the reaction chamber walls during that process. This, coupled with the reactivity of TMA with NH means that almost all of the reaction takes place at the chamber walls resulting in a very low growth rate.

The "goose-neck" injection tube (i.e. tube h, Fig. 10) configuration gave quite consistent flow profiles with high velocities except that the area of coverage under constant flow velocity was minimal. This meant that AlN films could be grown at a good rate with this system except that there was no uniformity in the film thickness throughout the sample surface.

The horizontal arm injection tube system (i.e. tube a, Fig. 10) provided a good compromise between the other systems and has been the only system to produce AlN films with a decent growth rate and with uniform substrate coverage. Its chief disadvantages are the lack of reproducibility of the injection flow profile (the slot is cut with a diamond saw blade and cut width does vary) and the production of AlN overgrowth around the slot edges which then falls onto substrate surfaces causing film irregularities.

2.2.3.2 Cooled reaction chamber growth. Some growth was attempted with a vertically upward directed injection system as

mentioned in Sec.2.2.3.1 but resulted in no AlN film growth although the chamber walls became completely coated with white AlN polycrystalline powder. Measurements of the chamber wall temperature during a growth run (at 1200°C susceptor temperature) reveal temperatures around the growth chamber of 280°C to 390°C. Wall temperature at the top of the chamber was 300°C with a vertical injection tube setup.

It was decided to build a cooling jacket for the chamber walls in an attempt to keep wall temperatures low and hopefully reduce reaction of the growth gases on the walls before reaching the substrate surfaces, (Fig. 11).

Several growth experiments were made in the water-cooled system with different injection systems and different gas flow rates. Of all the growth runs using a vertical injection type system, none produced any substantial film growth rate. Although the films were deposited very evenly, the maximum film thickness for the growth runs was only about 0.2 $\mu$  for a growth rate less than 0.2 $\mu$ /hr! There also were indications that after an initial growth of 0.1 $\mu$ , film growth is inhibited. Growth runs with the horizontal injection systems in the water cooled growth system, produced films with no difference from those grown under normal hot wall conditions.

The cooled chamber walls were still being covered with the white AlN powder although at a slower rate. This indicates that the TMA and NH gases probably are being heated by the radiant

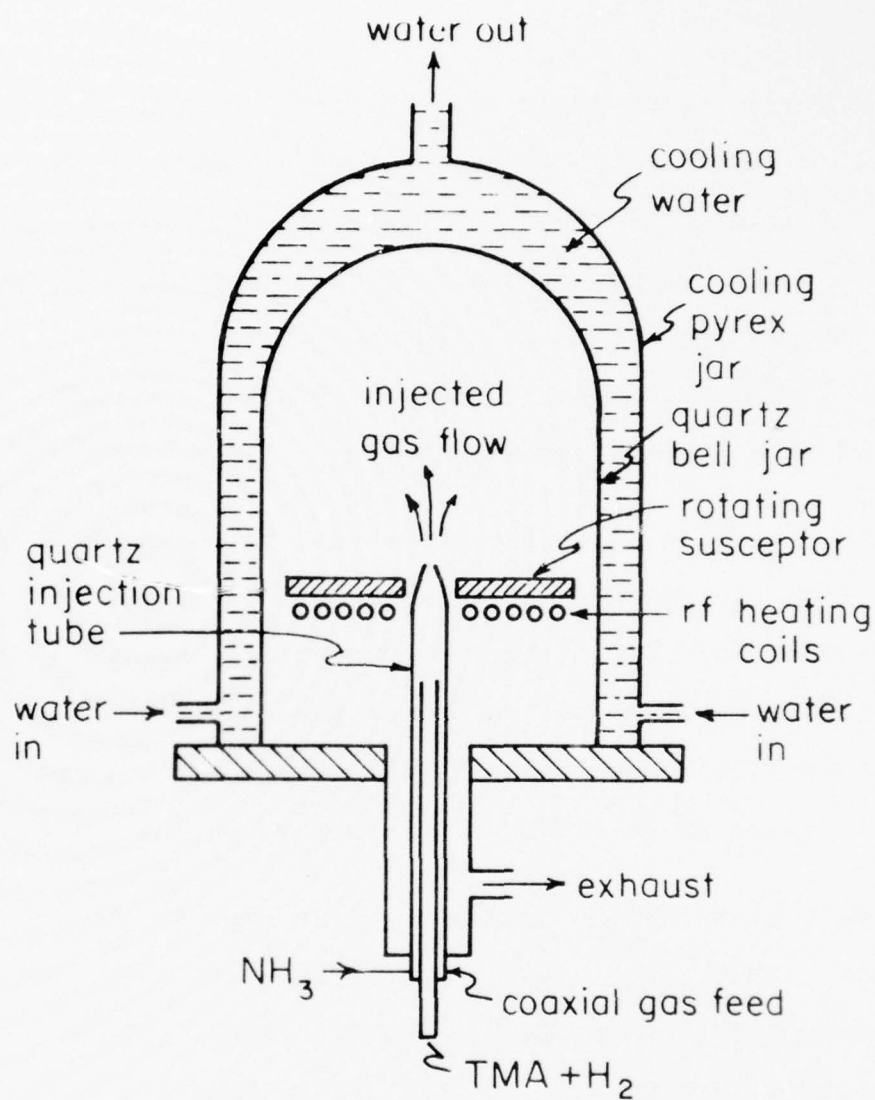


Figure 11. Water cooled reaction chamber.

heat of the susceptor within the chamber atmosphere and by their passage through the susceptor axis. They then react and deposit on the cool chamber walls.

2.2.3.3 Effect of Si upon AlN film growth. A growth run was made with a horizontal injection tube in which the horizontal arm containing the injection slot was stuffed with some quartz wool. This was an attempt to produce more resistance to the gas flow from the coaxial tube, so as to relieve some of the turbulence around the slot (thought to cause the AlN overgrowth) and to even out the flow profile across the slot.

The resultant AlN film growth was still uneven, but growth rate had increased considerably from a normal  $3\mu/\text{hr}$  to  $6\mu/\text{hr}$ . Examination of the film by scanning electron microscope techniques revealed that it was of good quality and piezoelectric measurements indicate films of slightly lower but still very good quality compared to films grown the regular way, (Figs. 12, 13).

Upon cleaning the apparatus after the growth run, it was noticed that the quartz wool in the injection tube had disintegrated into a white powdery mass. This led to the speculation as to what caused the increase in growth. Several possibilities came to mind, i) the quartz wool was actually creating a better mixture of the reactant gases and changing the flow character so that film growth is encouraged, ii) the quartz wool's large surface area actually created a catalytic action on the AlN formation, or iii) the Si or SiO in quartz actually

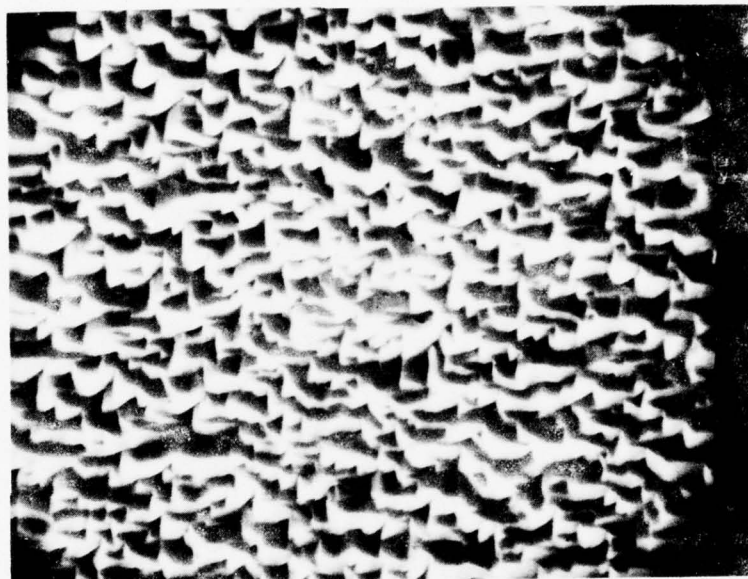


Figure 12. Surface morphology of AlN 09247140.



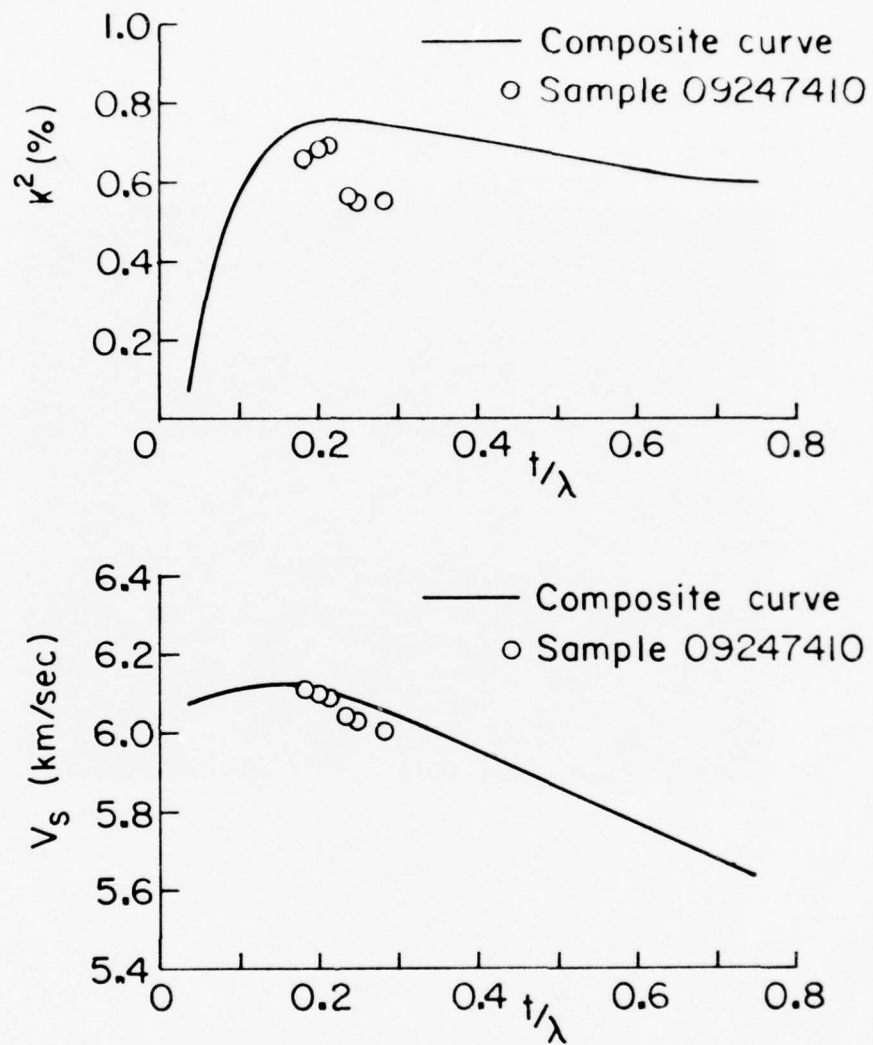


Figure 13. SAW measurement data of AlN 09247410.

promoted growth of AlN on sapphire.

In order to determine the action, if any, of Si on the growth of AlN,  $\text{SiH}_4$  was introduced into the injection flow in various amounts and the films were examined under a SEM [11], (Fig. 14). As can be seen by the SEM photograph of the as-grown film surface, the growth morphology has changed completely and shows no crystallinity in appearance.

It seems apparent then that, at least in the amounts injected, silicon is a contaminant to the growth of single crystal AlN and has no catalytic effect upon growth. Taking the quartz wool experiment and the results of  $\text{SiH}_4$  injection experiments together the conclusion can be made that growth of AlN on sapphire is highly dependent on flow profile of gases above growth surface. The quartz wool probably increased flow velocity through the injection slot causing increased film growth rate. The degradation in the film's characteristics was probably due to increased strain in film due to fast growth and/or due to Si or  $\text{SiO}$  contamination from the quartz wool.

### 2.3 Sample preparation.

2.3.1 Sample mounting for polishing. An important step in sample preparation is that of mounting samples onto polishing blanks. The usual procedure is to press samples onto a hot polish blank with melted wax as the adhesive. The assembly is allowed to cool with the samples under pressure. It has been



Figure 14. AlN growth with injected  $\text{SiH}_4$ .

found however, that the stresses developed with this procedure caused sample surfaces to warp. Subsequent dismounting of these samples with flat polished surfaces would release the mounting stresses and present a warped surface again.

Stresses developed in sample mounting can be attributed to i) mismatch between sample and blank surfaces, ii) temperature coefficients of expansion mismatch between sample and wax and/or polish block, iii) temperature coefficient of expansion mismatch between the AlN film and substrate and iv) the change in volume of wax that occurs upon cooling.

Steps taken to eliminate or reduce the problems were to eliminate the procedure of pressing samples down onto the polishing blank surface. Instead, the samples were allowed to float on the wax to ensure minimal mechanical stress. Further, the sample and block should be allowed to cool slowly.

Another problem arose when it was attempted to polish more than one wafer at a time. In this case, the additional problem was that of ensuring that all surfaces to be polished are coplanar. This was accomplished by placing a large quarter wave quartz optical flat on top of the wafers while the mounting wax was still liquid. After cooling, the flat was removed and the polish block assembly was carefully reheated up to a point where the wax was viscous enough to relieve local stresses introduced in the samples from the pressure of the mounting flat.

2.3.2 Film polishing. The as-grown AlN films were not suitable for piezoelectric measurements and for sample delivery. This was because the surface morphology of the as-grown films consist of scale-like facets, Fig. 7. The size and depths of the facets vary from  $0.5\mu$  for thinner films ( $1\mu$  or less) to  $5\mu$  for thicker films ( $10\mu$  or more). As the surfaces will have to support SAW of wavelengths as short as  $6\mu$ , it can be seen that the irregularities on the as-grown film surfaces are of the same order as the wavelength and would interfere with measurements. This means that the films have to be polished.

We have looked at various polishing methods, from pitch laps with Linde polishes to Syton polishing. The conclusion is that for final polishing in preparing the samples for SAW devices, Syton worked the best as it does not seem to leave any mechanical work damage on the surface that could cause interference with SAW propagation [12].

However, as we have mentioned earlier, Syton polishing with a Corfam pad causes rounding of the polishing surface. This was a problem in that it caused many thin films to polish off entirely at the edges before the center portions were polished sufficiently. The rounding effect also caused difficulty by preventing the samples from conforming to required thickness variation specifications.

Another problem noticed with Syton polishing was that the thicker films had a tendency to be polished more in random areas



than others. This is due to spurious nucleation from the injection tube that grew on the film surface towards the end of the growth run. The polish rate between coherent crystallites of the good film and the polycrystallites from spurious nucleation are different, causing uneven polishing.

This effect is reduced by inhibiting the chemical etching action of Syton (pH=2) on AlN films by neutralizing the fluid with HNO as monitored by a pH meter. We have found, using neutralized Syton (pH=7), that polish rates have decreased but now result in a more even surface profile. The reduced polish rate was a factor of four lower and consequently lengthened the polish time. The surfaces of the films do not show any mechanical abrasion damage from the partially neutralized Syton and are flatter with less rounding of the sample edges.

Since the amount of sub-surface mechanical damage could not be determined, any sample scheduled for AlN regrowth was polished with regular Syton.

#### 2.4 Film Characterization.

The AlN films were examined and characterized for their as-grown morphological appearance and piezoelectric properties. The results were correlated with growth and processing conditions in order to optimize the films for high frequency surface acoustic wave devices.

Previous studies of the surface morphology of as-grown AlN films on sapphire with a SEM together with piezoelectric characterization of the same films have established a correlation between the measured results and film surface character, [5]. Subsequent studies of as-grown AlN have thus made use of the SEM as a method of determining film quality.

2.4.1 Film thickness measurement. The AlN films were polished after SEM examination in preparation for application of aluminum interdigital transducers (IDT's) for piezoelectric characterization. Polishing was accomplished in either Syton or neutralized Syton (see Sec.2.3). Film thicknesses and thickness variations of the samples were monitored by examining the interference patterns created between the film surface and substrate surface under monochromatic light. (In this case, a sodium lamp). Absolute film thickness was measured by counting interference fringes across a wedge polished at the sample's edge to delineate a cross section of sapphire substrate and AlN film.

Surface flatness of the AlN/ $\text{Al}_2\text{O}_3$  composite was also monitored by examining interference patterns created between the AlN film surface and an optical flat placed on the sample. Close control of these two parameters, film thickness variation and surface flatness, is desired for applications to high frequency SAW devices.

2.4.2 Electrical characterization of films. Electrical measurements of IDT's on the AlN films were made to determine the

film's surface acoustic wave velocity and coupling coefficient. The low frequency capacitance of the transducers was measured and the average capacitance per finger pair,  $C_s$ , established for these particular IDT's. High frequency measurements were then made with a Hewlett Packard 8410A Network Analyzer. A reflected impedance plot of the transducer with swept frequency was reproduced onto a Smith chart, (Fig. 15). The resonant loop was centered on the Smith chart by series inductor tuning. The tuning is normally achieved with an inductor coil, but in this case, at the high frequency of operation and capacitance of the IDT, adjusting the length of the gold connecting wires was sufficient for tuning purposes.

The peak radiation resistance  $R_a$  of the transducer is determined by the difference between the peak value and the electrode and coil conduction loss at low frequencies, where no acoustic interaction is present. Frequency at resonance,  $f_0$ , is measured where the peak radiation resistance occurs. The electromechanical coupling coefficient,  $K^2$ , is defined by the equation,

$$K^2 = \frac{\pi^2}{2} f_0 C_s R_a$$

where  $f_0$  = frequency of maximum  $R_a$

$R_a$  = radiation resistance

$C_s$  = capacitance per finger pair.

The surface wave phase velocity,  $V_s$ , is determined by the synchronous radiation condition that occurs at resonance, where

NAME	TITLE	AWG. NO.
SMITH CHART FORM 530-7560-N	AIN 012176 IDT#4/2 $t/\lambda = 0.101$	DATE 2/3/76
GENERAL RADIO COMPANY, WEST CONCORD, MASSACHUSETTS		

IMPEDANCE OR ADMITTANCE COORDINATES

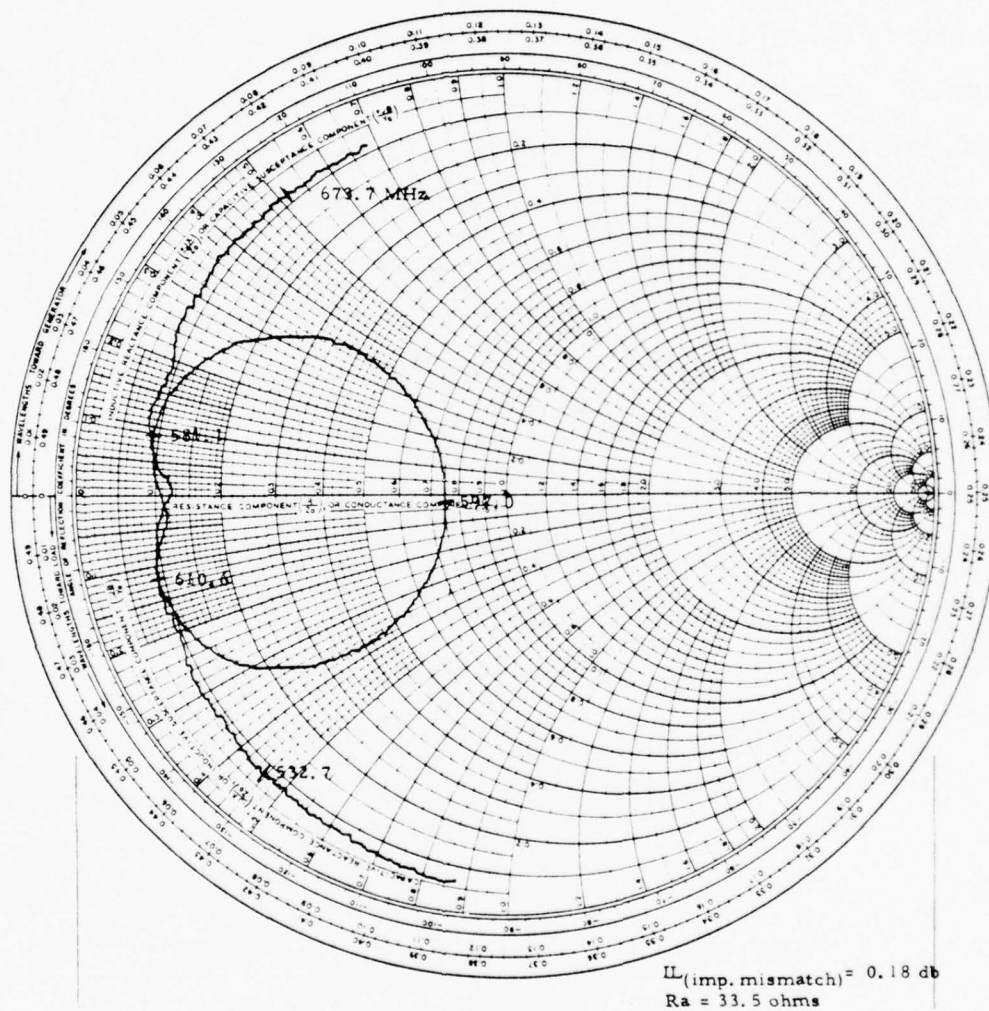


Figure 15a. Reflected impedance Smith chart plots.



NAME	TITLE AIN 012176 IDT #5/2	$t/\lambda = 0.107$	DWG. NO.
SMITH CHART FORM 530-7560-N	GENERAL RADIO COMPANY, WEST CONCORD, MASSACHUSETTS	DATE 2/3/76	

IMPEDANCE OR ADMITTANCE COORDINATES

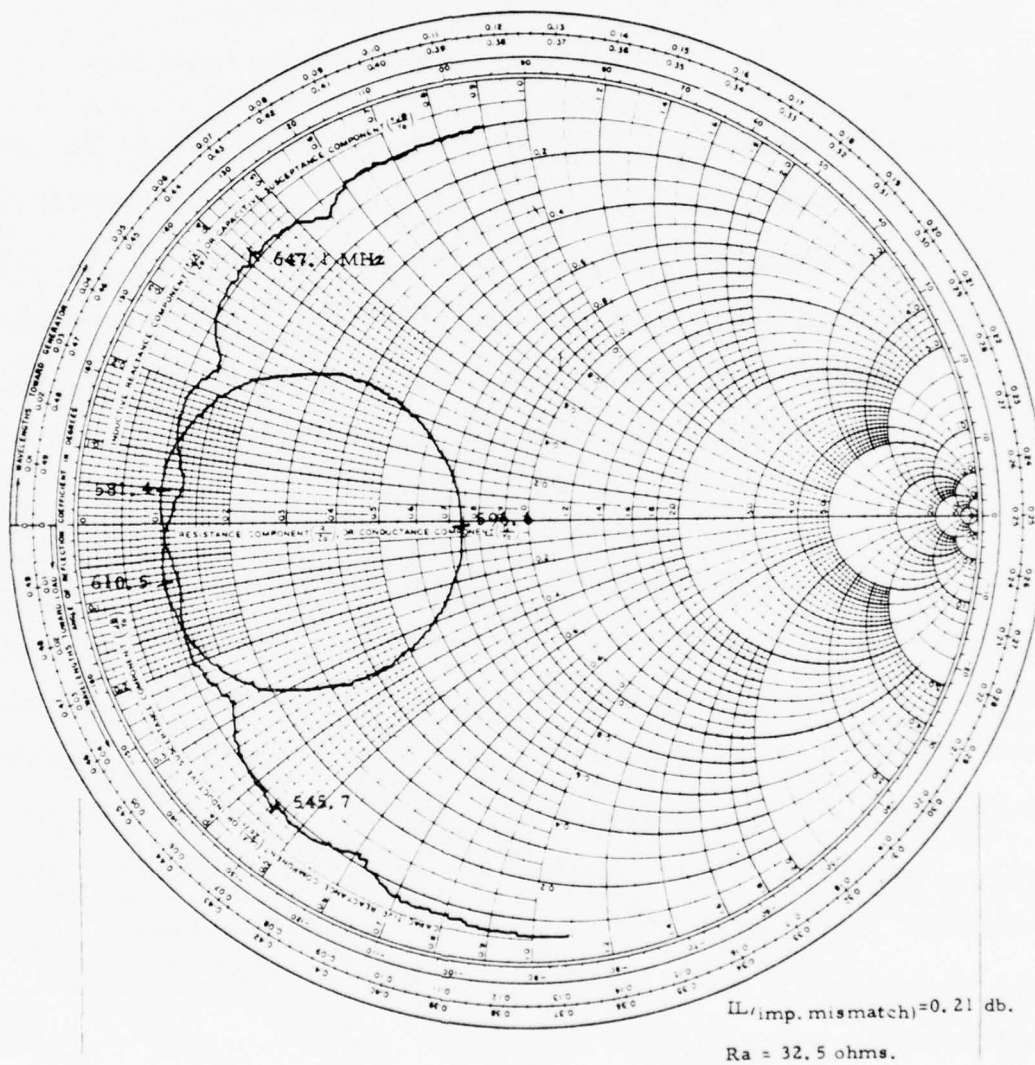


Figure 15b. Reflected impedance Smith chart plots.



the acoustic wavelength matches the transducer periodicity. The velocity  $V_s$  is given by,

$$V_s = f_0 \lambda$$

where  $f_0$  = frequency of maximum Ra  
= transducer electrode periodicity.

2.4.2.1 Discussion of  $K^2$  and  $V_s$  measurements.  $K^2$  and  $V_s$  were measured for some samples and plotted against film thickness divided by transducer periodicity,  $t/\lambda$ , (Figs. 16, 17). Superimposed upon the  $K^2$  measurements is a composite curve of some previous samples, [5]. (The relative values of  $K^2$  of these previous samples have been revised to reflect more accurate  $C_s$  measurements.)

An examination of the data points for the three samples measured revealed a significant difference in the values compared to the composite curve at some  $t/\lambda$ 's. For sample 012176,  $K^2$  values at  $t/\lambda < 0.1$  are significantly higher than those obtained from previous samples, while sample 112475 showed lower  $K^2$  and  $V_s$  values over all points measured. All three samples showed a significant decrease in  $K^2$  and  $V_s$  values with increasing  $t/\lambda$ . Growth conditions for these three samples together with a previous sample used for the composite curve are tabulated in Table I. The surface morphologies of the four samples are also shown in SEM photos in Fig. 18.

Studies in silicon on sapphire devices have shown the

TABLE I Growth Conditions of Some ALN Samples

Sample No.	Growth Temp.	Inj'n Tube	Flow rates	Growth rate	Performance
052374	1215°C	1.7"x0.021"	H <sub>2</sub> - 8 $\ell$ /m	450 Å/m	V <sub>s</sub> = 6115 Km/s K <sup>2</sup> = 0.68 %, at t/λ = 0.175
			TMA - 0.030 $\ell$ /m		
			H <sub>2</sub> add - 0.4 $\ell$ /m		
			NH <sub>3</sub> - 1.2 $\ell$ /m		
112475	1205°C	1.7"x0.022"	H <sub>2</sub> - 8 $\ell$ /m	480 Å/m	V <sub>s</sub> = 5.90 Km/s K <sup>2</sup> = 0.45% at t/λ = 0.15
			TMA - 0.035 $\ell$ /m		
			H <sub>2</sub> add = 0.5 $\ell$ /m		
			NH <sub>3</sub> = 1.2 $\ell$ /m		
012176	1216°C	1.7"x0.042	H <sub>2</sub> = 6.3-8.3 $\ell$ /m	70 Å/m	V <sub>s</sub> = 6.1 Km/s K <sup>2</sup> = 0.7% at t/λ = 0.16
			TMA = 0.030 $\ell$ /m		
			H <sub>2</sub> add = 0.5 $\ell$ /m		
			NH <sub>3</sub> = 1.2 $\ell$ /m		
021076	1204°C	1.7"x0.042	H <sub>2</sub> = 8.3 $\ell$ /m	80 Å/m	V <sub>s</sub> = 6.1 Km/s K <sup>2</sup> = 0.7% at t/λ = 0.2
			TMA = 0.030 $\ell$ /m		
			H <sub>2</sub> add = 0.3 $\ell$ /m		
			NH <sub>3</sub> = 1.2 $\ell$ /m		

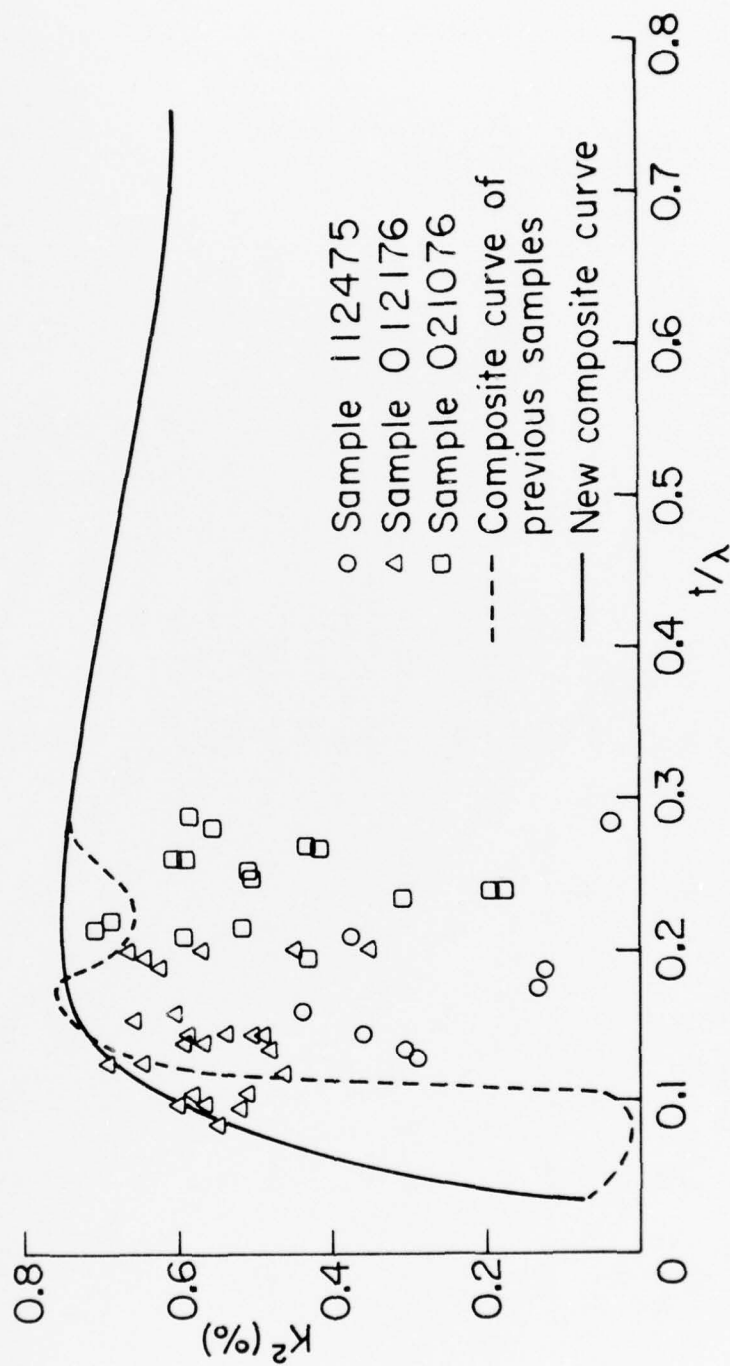


Figure 16. Electromechanical coupling constant,  $K^2$ , versus  $t/\lambda$ .

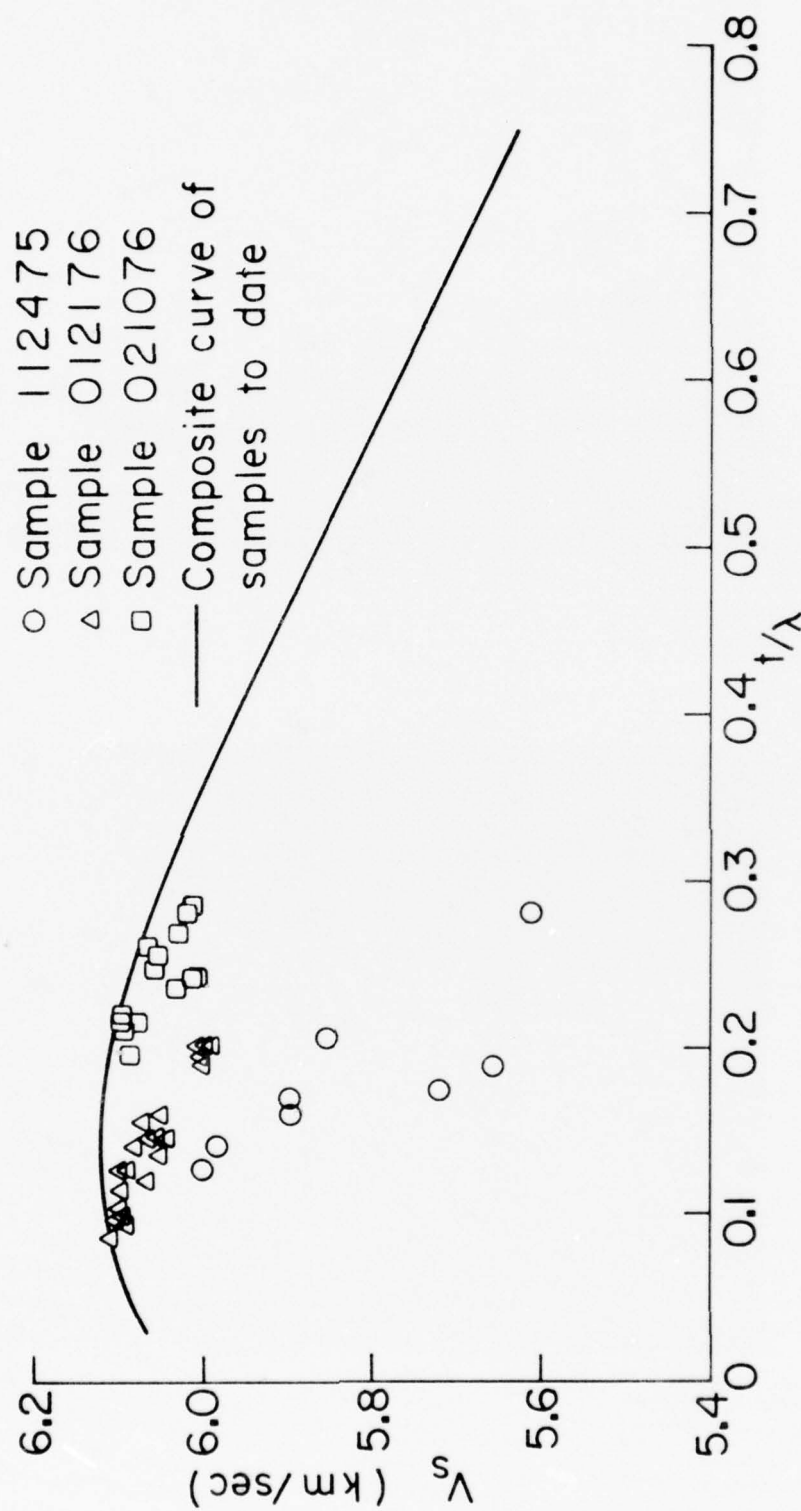
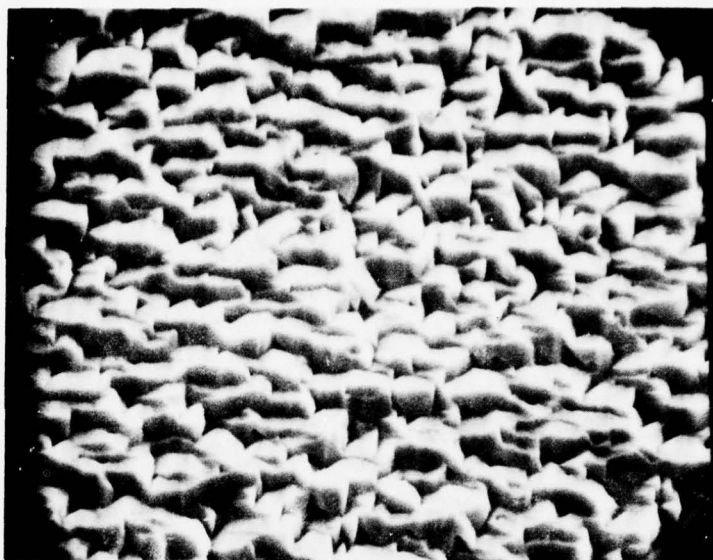


Figure 17. Surface acoustic phase velocity,  $V_s$ , versus  $t/\lambda$ .



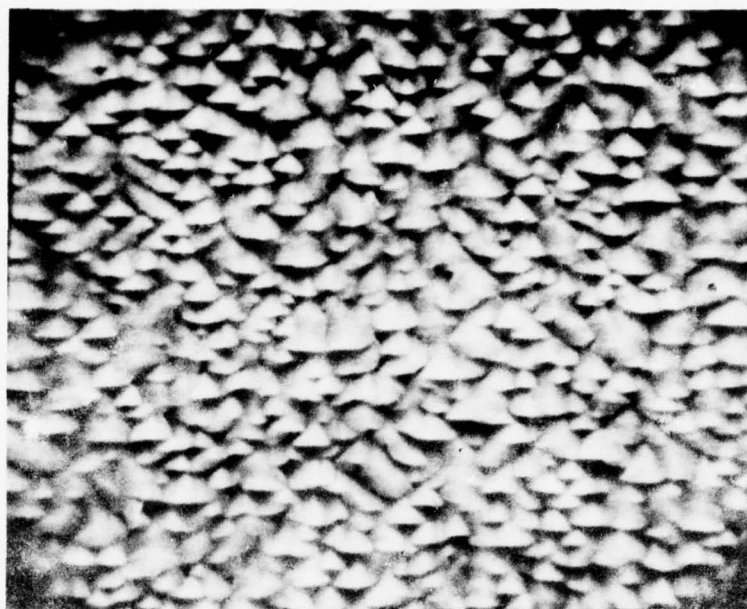
a)



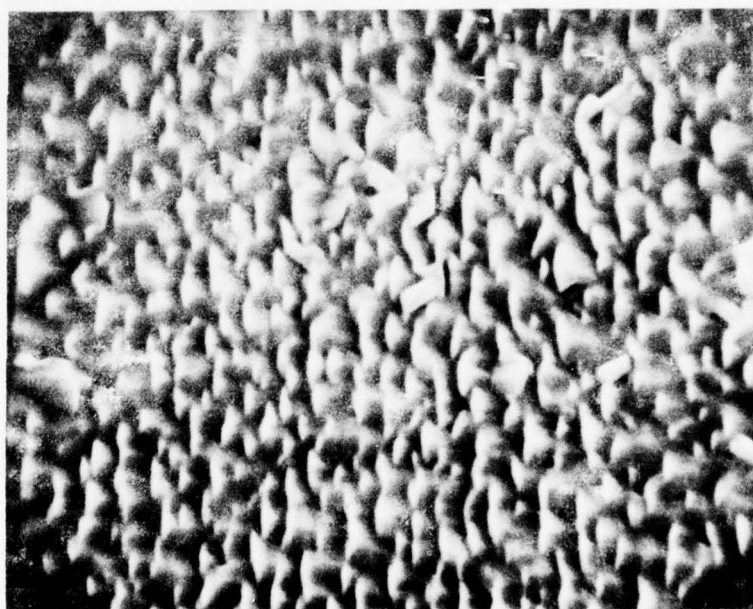
b)

Figure 18. Surface morphologies of some AlN samples.





c)



d)

Figure 18. Growth morphologies of some AlN samples.

interfacial region to be composed of an intermediate compound of silicates, the extent of which seems to be influenced by the density of initial growth sites, [14]. A similar situation can be seen to exist in the AlN/Al<sub>2</sub>O<sub>3</sub> growth system. If AlN reacts with Al<sub>2</sub>O<sub>3</sub> the substrate surface during initial nucleation stages to form an intermediary compound, then the film thickness at which AlN forms a closed layer on the surface determines when reaction between AlN and Al<sub>2</sub>O<sub>3</sub> is suppressed and hence determines the piezoelectrically inactive region thickness. Growth rates, which are determined by gas flow velocity, temperature [15] and reactant input, also are reflected in crystallite size and hence nucleation density. The SEM photographs of the as grown AlN film surfaces show crystallite sizes that vary directly with growth rate. Higher growth rates then, would produce films with thicker layers of piezoelectrically inactive material at the interface. The effects of this layer can be clearly seen by measuring the samples with different wavelength transducers and seeing the change of the K<sup>2</sup> values at low t/λ's.

The decrease in measured SAW parameters for larger t/λ's for the present samples can be explained by the fact that film growth conditions change after a period of time in the growth apparatus due to the accumulation of AlN polycrystalline powder around the injection slot. Experience has shown that this generally occurs around two hours into the growth run. With decreasing growth rates, the time limitation does not change, hence the film thickness (or t/λ) at which degradation of

piezoelectric activity begins to occur decreases. SAW parameters for sample 021076 (Fig. 18), before and after further polishing to remove surface material, clearly show the degradation of film quality as film thickness increases beyond a certain point.

The inferior quality of sample 112475 as revealed by the SAW parameter measurements and its surface morphology can be explained by the fact that a leak in the hydrogen purifier was discovered around the time this sample was grown. The resultant decrease in purity of the inlet gases undoubtedly contaminated the growth system and adversely affected the quality of film grown.

2.4.2.2 Surface-wave group velocity. The surface wave group velocity or propagation velocity,  $V_g$ , is related to surface wave phase velocity,  $V_s$ , by the relation,

$$V_g = dV_s/d(t/\lambda) + V_s$$

$V_g$  is calculated from the composite  $V_s$  curve and is shown in, Fig. 19. Propagation velocity for several samples is calculated by measuring triple transit signal delay between IDT's as revealed in the fine structure of a transmission plot versus swept frequency at resonance, Fig. 20. The plot is repeated in the same figure with absorber material between IDT's to confirm SAW transmission. Error bars in  $t/\lambda$  regime for the measured points in Fig. 19, are to reflect the difference in film thickness through which the acoustic waves travel between the transducers.

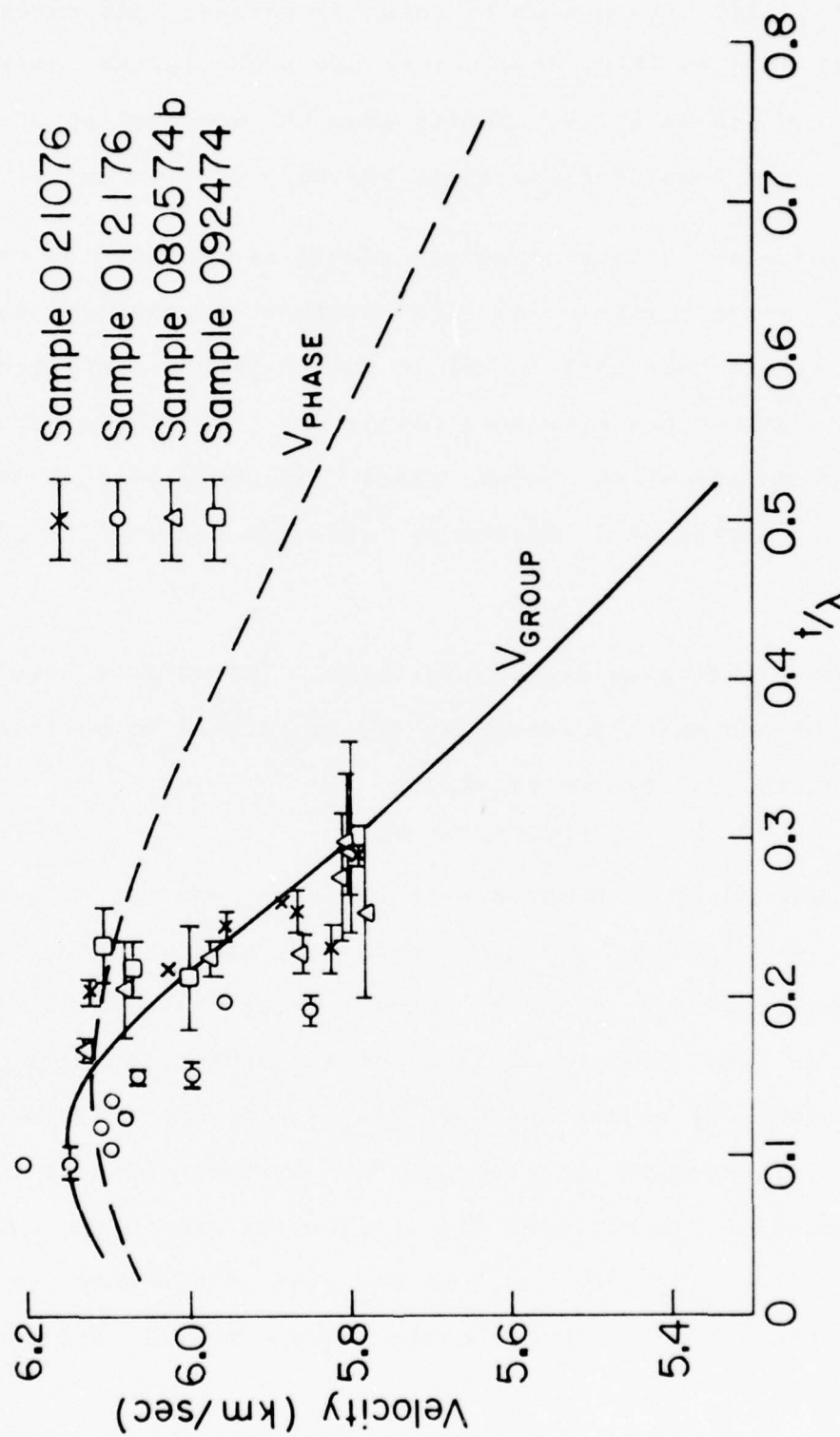


Figure 19. Surface wave group and phase velocities versus  $t/\lambda$ .

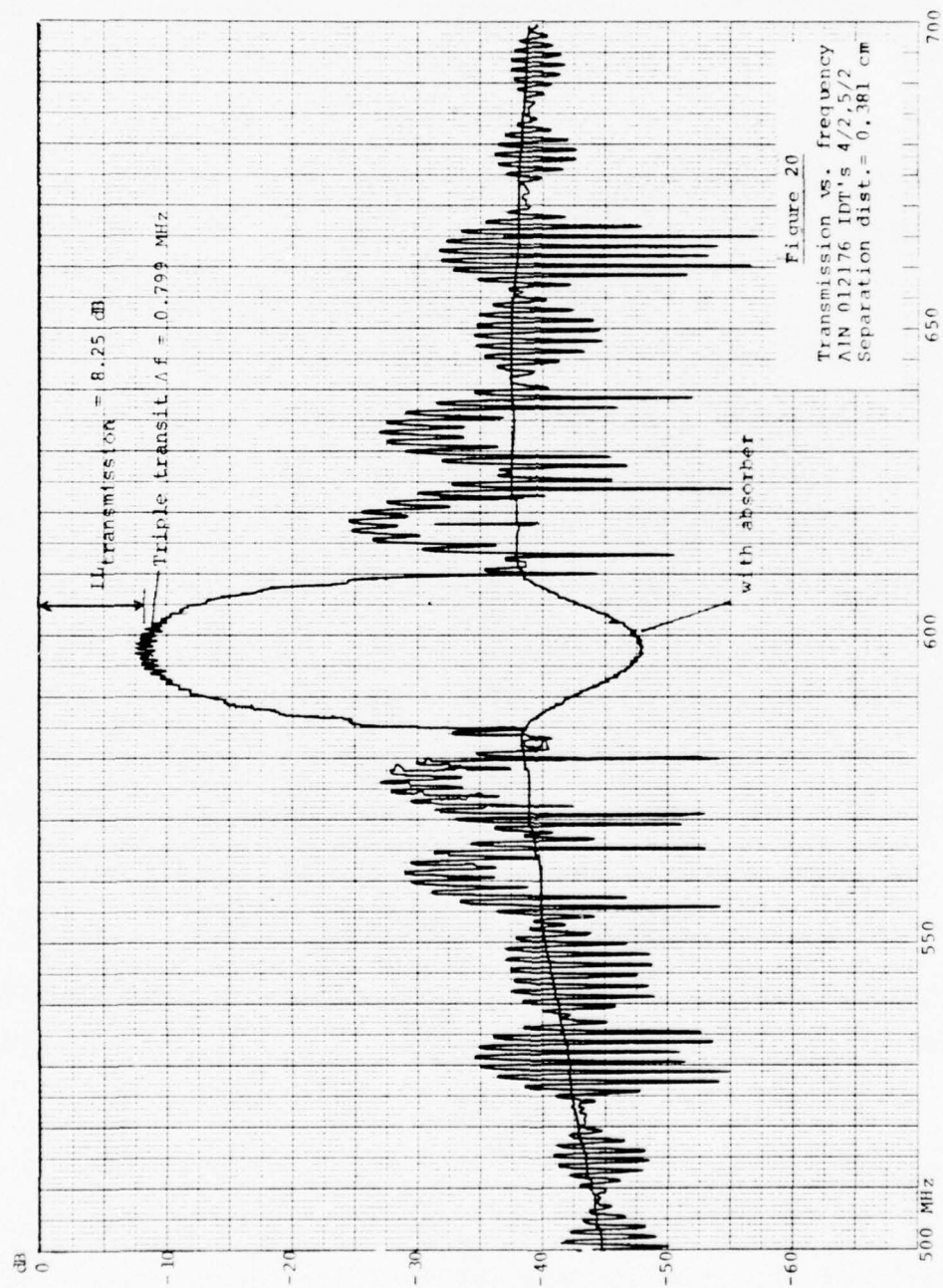


Figure 20. SAW transmission versus frequency.



2.4.2.3 SAW attenuation in the film. Insertion loss at resonance enables SAW attenuation in AlN to be calculated. For a conventional IDT delay line,

$$\begin{aligned} \text{IL(material)} &= \text{IL(transmission)} - \text{IL(transducers)} \\ &\quad - \text{IL(mismatch)} \end{aligned}$$

where

$$\text{IL(transducers)} = 6\text{dB.}$$

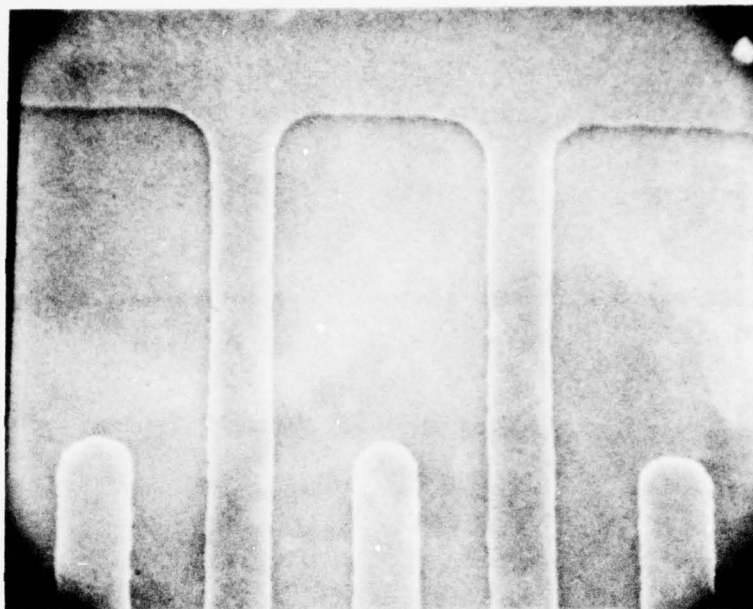
$$\text{IL(mismatch)} = 10 \log 4r/(1 + r)^2$$

$$\text{where } r = |Z_t/Z_\ell|$$

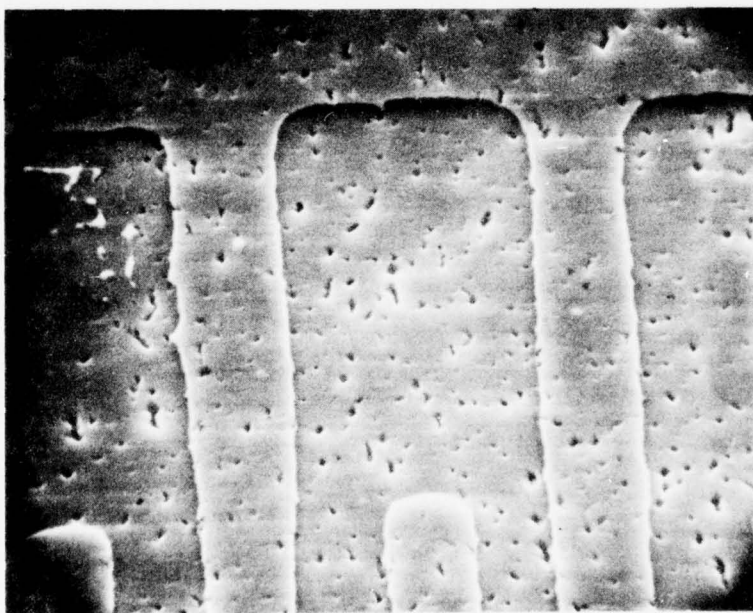
$$\text{and } Vg = 2d\Delta f$$

$$\text{where } d = \text{IDT separation distance.}$$

Using the above equations and data from Figs. 15 and 20, sample 012176 has  $Vg = 6.09 \text{ km/sec.}$  and a SAW attenuation =  $2.93 \text{ dB}/\mu\text{S.}$  At high frequencies, SAW parameter measurements have been shown to be highly sensitive to surface finish and material quality [12]. This is also true for AlN films where the surface morphology contains crystallites and defects large enough to require extensive polishing to remove pits from the surface. Referring to the  $K^2$  and  $Vs$  measurements for AlN 012176 at  $t/\lambda = 0.2$  in Fig. 16, it can be seen that there is a large difference in piezoelectric activity at different regions of the sample. This is because of uneven growth rates caused by uneven gas flows from the horizontal injection tube. SEM examination of the polished film surfaces where some IDT's are located, show the presence of a large number of pits and defects (Fig. 21). The defect density of the film surface around the IDT's has been

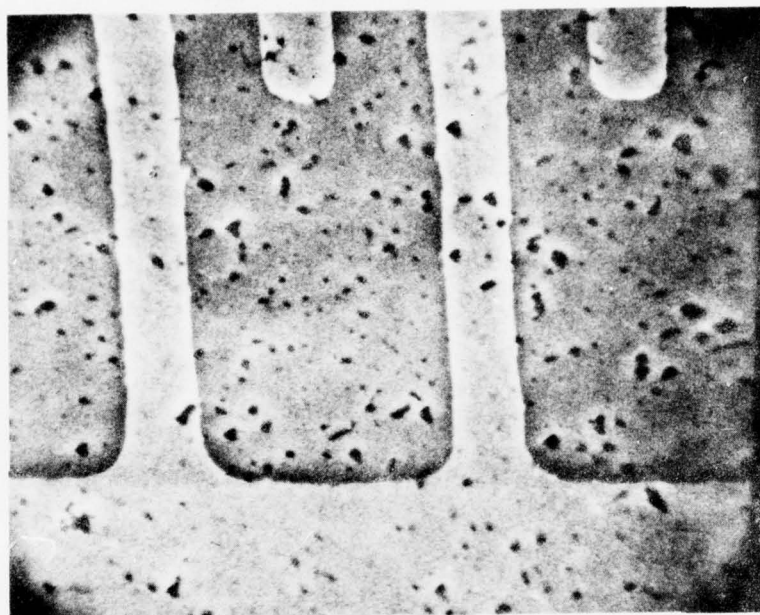


a)



b)

Figure 21. Character of polished AlN film surfaces under some IDT's.



c)

Figure 21. Character of polished AlN film surfaces under some IDT's.

correlated with degradation of piezoelectric activity and increased SAW attenuation in the material.

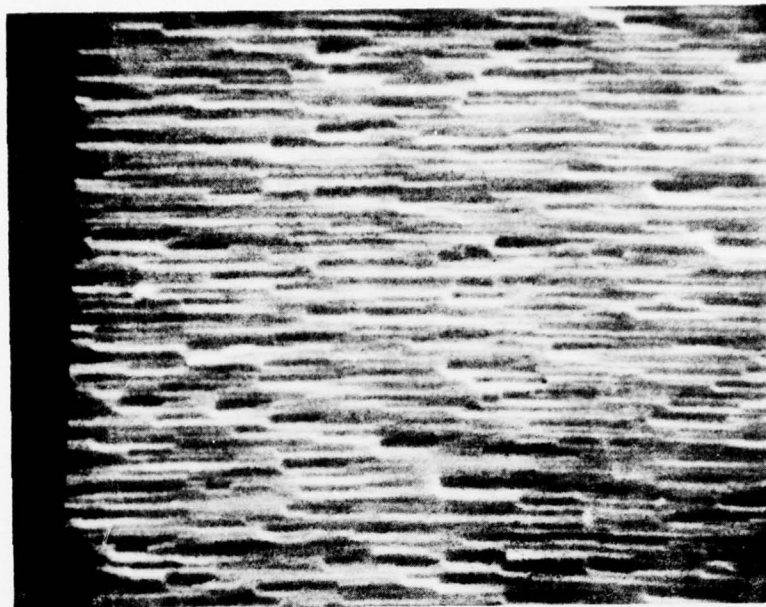
#### 2.4.3 Other experiments.

2.4.3.1 Film etching. Some AlN film surfaces were etched with NaOH and examined under the SEM. This revealed preferential etching of the surface (Fig. 22). As etching rate increases along a region of higher strain or of higher impurity content (i.e. grain boundaries), the technique is useful for revealing the state of strain and coherence of the film surface. From Fig. 22 we can see the etched surfaces become progressively rougher with increasing film thickness crystallite size and spurious nucleation density.

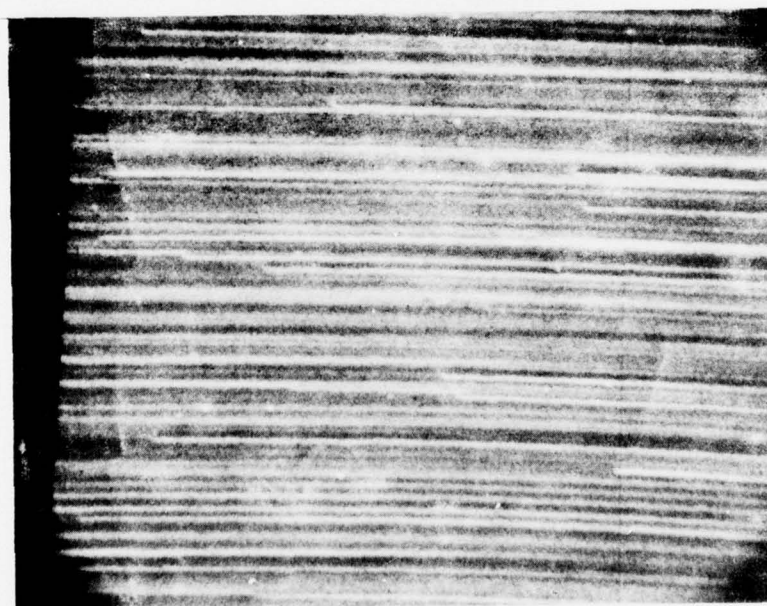
Comparing the SEM photographs of the etched AlN surface with as-grown AlN surfaces during transition from "scale" to "ridge" growth (Fig. 23) along with the knowledge of the growth orientation of AlN on Al<sub>2</sub>O<sub>3</sub> (11 $\bar{2}$ 0/01 $\bar{1}$ 2) [5], it can be seen that etching reveals the AlN (01 $\bar{1}$ 0) planes. As has been reported, accurate alignment of IDT's on AlN is important for optimal SAW propagation in a AlN/Al<sub>2</sub>O<sub>3</sub> composite [15]. This etching method can be a way of determining AlN film orientation.

2.4.3.2 Sample bowing due to thermal affects. As mentioned before (See 2.1) stresses introduced into the samples from unequal temperature coefficients of expansion and lattice constants of sapphire and AlN are manifested in substrates bowing





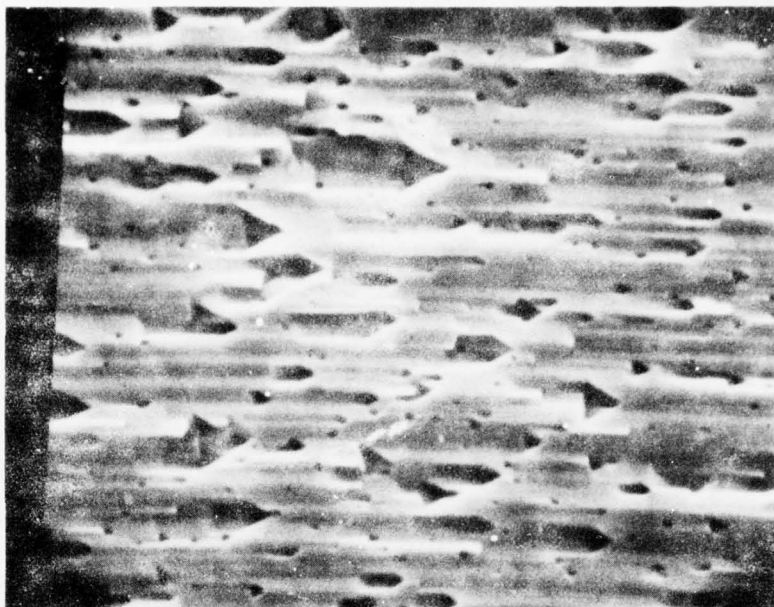
a)



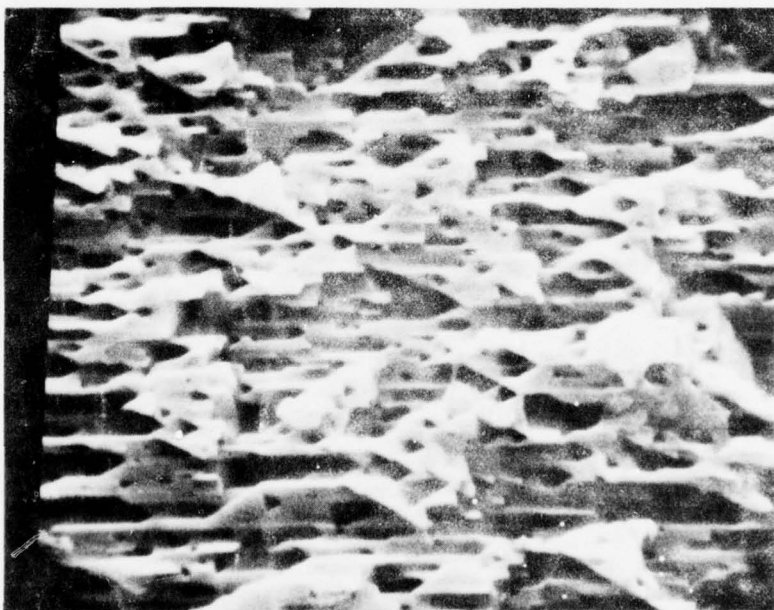
b)

Figure 22. Some etched AlN surfaces.





c)



d)

Figure 22. Some etched AlN surfaces.

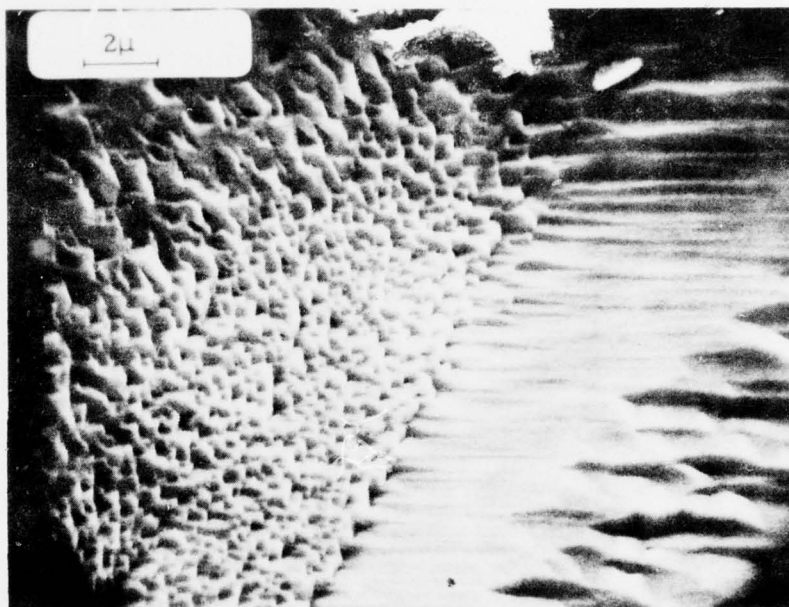


Figure 23. Growth transition area on AlN film.

and even cracking in extreme circumstances. Calculations have been made for the amount of "bowing" due to thermal stresses introduced into an  $\text{AlN}/\text{Al}_2\text{O}_3$  composite and show that, using temperature coefficients to the first-order [1], a linear dependence of "bowing" with respect to film thickness is found for cases where film thickness is much less than substrate thickness [16]. For a growth temperature of  $1200^\circ\text{C}$ , and substrate dimensions  $1.000'' \times 0.354'' \times 0.040''$ , surface "bowing" due to stresses along the sample length is 0.45 AlN film thickness. This figure is in fair agreement with the "bowing" actually observed in the prepared samples from counting the difference in Na interference fringe counts of the surfaces of several samples with different film thickness and from the same sapphire.

2.4.3.3 Temperature coefficient of delay. As for the surface wave phase velocity and coupling coefficient, temperature coefficient of delay of the surface wave should also be a function of  $t/\lambda$  at thin film thicknesses because of the influence of the substrate upon the AlN's acoustic properties. We would expect that the coefficient of delay of the composite material ( $\text{AlN}/\text{Al}_2\text{O}_3$ ) to progress from the sapphire value to that of AlN's value as film thickness increases.

Temperature coefficient measurements have been made [11] on several AlN C-axis propagating delay lines for the temperature range  $20\text{--}75^\circ\text{C}$  (Fig. 24). The coefficient value falls from that

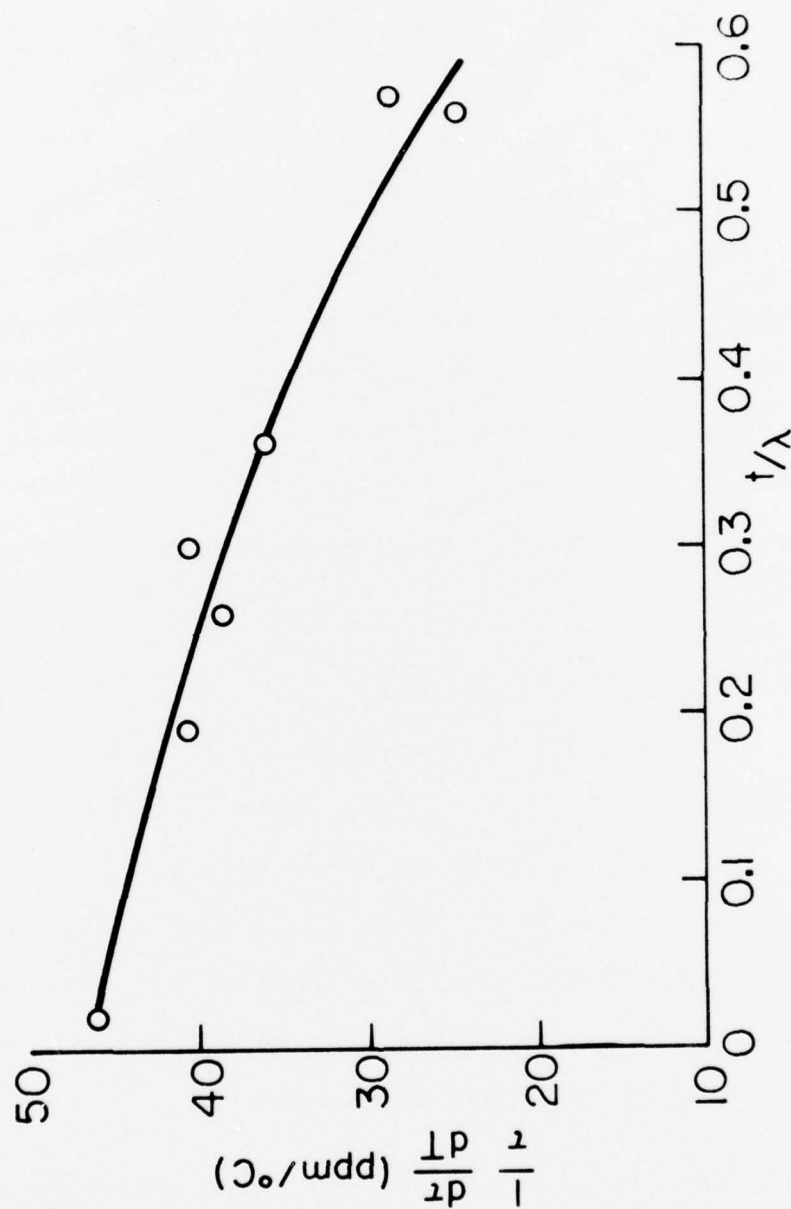


Figure 24. Temperature coefficient of surface wave delay versus film thickness.

slightly below sapphires's theoretical value of 59.3 ppm/ $^{\circ}$ C to 13 ppm/ $^{\circ}$ C for  $t/\lambda=0.66$  as film thickness increases. If aluminum nitride has a negative coefficient of delay we can expect the composite structure to exhibit zero temperature coefficient at some higher  $t/\lambda$ . Further measurements have to be made on thicker films or with higher frequency delay lines to determine if this actually is true.



### 3.0 CONCLUSIONS AND RECOMMENDATIONS

#### 3.1 Conclusions.

An important factor in the fabrication of AlN/Al<sub>2</sub>O<sub>3</sub> samples with physical dimensions conforming to required contract specifications is the condition of the substrates received. Substrate orientation and surface preparation are sometimes required.

Several growth injection systems have been examined with the conclusion that films of optimum quality and consistency are achieved using a horizontal slotted arm injection system.

Film and substrate polishing in preparation for AlN growth was best done with a chemo-mechanical polish which produces a surface with little mechanical damage.

Some AlN/Al<sub>2</sub>O<sub>3</sub> samples of the required specifications have been fabricated and delivered to the contractor in fulfillment of the program goals.

The approach taken in the latter stages of the program was to grow thin, good quality AlN films on flat substrates, and prepare surfaces with a minimal chemo-mechanical polish. The advantages of this approach are:

- i) The minimization of sample "bowing" due to film/substrate stress.
- ii) Reduction of growth time required per sample.

- iii) Reduction of crystallite size and hence polish time.
- iv) Achievement of maximum SAW propagation velocity for reasonable electromechanical coupling.

The disadvantages are the potential interference of the interfacial region with piezoelectric performance and the non-zero thermal coefficients of delay.

### 3.2 Recommendations for further work.

A more theoretical study into the growth and reproducibility problems of fabricating AlN epitaxial films on sapphire substrates for SAW devices is required to support the empirical results obtained in this program. Emphasis should be placed on the investigation of the gas reaction kinetics of AlN growth from CVD techniques together with close monitoring of the results with electrical and physical examination of the fabricated samples.

Further investigation into the growth of thicker good quality AlN films is required to facilitate the characterization of the temperature coefficient of delay of the composite sample. The possibility of producing a zero temperature coefficient piezoelectric composite that can operate at higher frequencies can then be determined.

Some preliminary work has shown that AlN could serve as a useful substrate material for the growth of other compounds (Ga<sub>2</sub>N, ZnO, Si) and work towards this end should be pursued.

The studies of the piezoelectric behaviour of the AlN/sapphire composite suggest that this material would be applicable to bulk shear wave transduction as well.

## REFERENCES

1. W.M. Yim and R.J. Paff, J. Appl. Physics.  
45,1456(1974).
2. M.T. Duffy, C.C. Wang, G.D. O'Clock Jr., S.H.  
McFarlane III and P.J.Zanzucchi, J. Elecron.Mater,. 2,  
359(1973).
3. W.M. Yim, E.J. Stofko, P.J. Zanzucchi, J.I. Pankove,  
M. Ettenberg and S.L. Gilbert, J. Appl. Physics.  
44, 292(1973).
4. M.P. Callaghan, E.Patterson, B.P. Richards and  
C.A.Wallace, J.Crystal Growth, 22, 85(1974).
5. J.K. Liu, K.M. Lakin and K.L. Wang, J. Appl. Physics.  
46, 3703(1975).
6. Syton is a Monsanto trademark.
7. Corfam is a Dupont trademark.
8. M.T. Duffy, C.C. Wang, "Piezoelectric Aluminum  
Nitride films", U.S. Government Report No.  
AFCRL-TR-74-0559.
9. W. Griffel, "Handbook of formulas for Stress and  
Strain", 175.(Ungar,1966).
10. E. Wiberg and A. Bolz, FIAT-Rev., 24, 160(1950).
11. J.K. Liu, R.B. Stokes and K.M. Lakin, Proc. 1975 IEEE  
Ultrasonics Symposium, 234(1975).
12. R.C. Williamson, Proc.1974 IEEE Ultrasonics

Symposium, 321(1974).

13. H. Schlotterer, J. Vac. Sci. Tech. 13, 29, (1/76).
14. A.J. Noreika, and D.W. Ing, J. Appl, Physics, 39, 5578(11/68).
15. K.M. Lakin, J.K. Liu and K. Wang, Proc.1974 IEEE Ultrasonics Symposium, 302(1974).
16. R.B. Stokes, private communication.



# *MISSION of Rome Air Development Center*

*RADC plans and conducts research, exploratory and advanced development programs in command, control, and communications (C<sup>3</sup>) activities, and in the C<sup>3</sup> areas of information sciences and intelligence. The principal technical mission areas are communications, electromagnetic guidance and control, surveillance of ground and aerospace objects, intelligence data collection and handling, information system technology, ionospheric propagation, solid state sciences, microwave physics and electronic reliability, maintainability and compatibility.*



Printed by  
United States Air Force  
Hanscom AFB, Mass. 01731